Eikonomics: Radiomics, Genomics, Cancer; Diagnostic and Prognostic

Terrence P McGarty
White Paper No 174
April 2020

εικονίζω, a verb, means to picture, to image, to visualize in Greek and the neologism "Eikonomics" means the art of visualizing or envisaging. It may not be the best to begin a document of this type by inventing a new word but it may have some merit as we proceed. In the analysis of a patient where we seek to ascertain if they have some form of malignancy, we all too often deal with images, icons if you will of how the disease is presented to us. It is not the symptoms but the radiological image, the ultrasound image, the cytological or histological image. The image is limited in a sense by the tools available. Cytologically we have the resolution, the results of stains, of antibodies, and even of electron microscopic analyses.

Notice

This document represents the personal opinion of the author and is not meant to be in any way the offering of medical advice or otherwise. It represents solely an analysis by the author of certain data which is generally available. The author furthermore makes no representations that the data available in the referenced papers is free from error. The Author also does not represent in any manner or fashion that the documents and information contained herein can be used other than for expressing the opinions of the Author. Any use made and actions resulting directly or otherwise from any of the documents, information, analyses, or data or otherwise is the sole responsibility of the user and The Author expressly takes no liability for any direct or indirect losses, harm, damage or otherwise resulting from the use or reliance upon any of the Author's opinions as herein expressed. There is no representation by The Author, express or otherwise, that the materials contained herein are investment advice, business advice, legal advice, medical advice or in any way should be relied upon by anyone for any purpose. The Author does not provide any financial, investment, medical, legal or similar advice in this document or in its publications on any related Internet sites.

Furthermore, this document contains references to and quotes from papers and documents under the premise of Fair Use in order to present ideas and understandings in context. The Author has attempted to make any and all references to such material separate from those of the author per se and has referenced the source expressly in all cases. These documents are for the dissemination of ideas and have no commercial intent. The Author would appreciate any communications relating to these documents and these should be sent to:

tmcgarty@telmarc.com.

Table of Contents

1 Introduction 4
1.1 Basic Constructs 5
1.2 Some Statistics 6
1.2.1 Analog Variables 6
1.2.2 Digital Variables 7
1.3 Summary 13
2 Imaging 15
2.1 US 15
2.2 CAT 16
2.3 MRI 17
2.4 2D, 3D, or 4D Imaging 17
2.5 Cytology and Histology 17
3 mpMRI Options: Image Analyses 20
3.1 General Assumptions 20
3.2 Generalized Metrics 21
3.3 Cluster Analyses 21
3.4 Pattern Recognition 22
3.5 Classifications; Supervised and Unsupervised 22
3.6 Neural Nets 28
4 Genomics Integrated 33
4.1 DNA 33
4.1.1 Mixed Cells 33
4.1.2 Single Cells 33
4.2 RNA 34
4.3 miRNA 34
5 Cancers 37
5.1 Prostate 37
5.1.1 The PSA Test 37
5.1.2 mpMRI 42
5.1.3 US 49
5.1.4 Biopsy 49
5.1.5 Genomics 50
5.2 Breast 52

5.2.1 Classic Methods 52
5.2.2 mpMRI 53
5.2.3 Biopsy and Images 55
5.2.4 Neural Nets 58
5.3 Thyroid 62
5.3.1 Ultrasound 62
5.3.2 Genomic Analyses 66
5.3.3 Cytological Analyses 67
5.3.4 Expert Systems 78
5.4 Summary 79
6 Observations 80
6.1 RNA Markers 80
6.2 Neural Networks and Dimensionality 80
6.3 Speech Recognition to Image Recognition 81
7 References 82
8 Index 90

1 INTRODUCTION

εικονίζω, a verb, means to picture, to image, to visualize in Greek and the neologism "Eikonomics" means the art of visualizing or envisaging. It may not be the best to begin a document of this type by inventing a new word but it may have some merit as we proceed. In the analysis of a patient where we seek to ascertain if they have some form of malignancy, we all too often deal with images, icons if you will of how the disease is presented to us. It is not the symptoms but the radiological image, the ultrasound image, the cytological or histological image. The image is limited in a sense by the tools available. Cytologically we have the resolution, the results of stains, of antibodies, and even of electron microscopic analyses. The questions we then seek to examine are then:

1. How can we apply sophisticated computer processing to enhancing the multiplicity of imaging techniques?

2. Which of the available techniques offer the best options in diagnosis and prognosis. For example, should we rely upon existing metrics and then try to computerize them or should we seek such options as neural networks wherein we may have no idea what the underlying metric may be.

3. Can we, via the computerized approaches, seek enhanced correlative methods to blend the methodologies?

4. Where and how can we integrate genomic information and seek to correlate them with the other data sets?

5. Should the exiting metrics for current imaging analyses be integrated into advanced neural networking methodologies. Namely, a multiplicity of metrics or observables have been identified and incorporated over the past century in radiology and histology to identify key disease states. Should we use these as starting points or should they just be abandoned and let the neural nets just work their wonders?

6. In Eikonomics, should we seek dispositive answers or just useful leads?

7. How best should we try to integrate a multiplicity of imaging media?

Imaging has been a separate path in the diagnosis and treatment of cancers. It has net generally been an integrated element in this process. The imaging modalities are often independent of the many insights in the areas of genomics and immunotherapy. The imaging specialist generally utilizes a standard set of tool to perform independent assessments of putative lesions, trying to localize and identify them back to the individuals doing the assessment and treatment.

In this note we try to examine the potential for imaging, understood as radiomics, as a tool which can be integrated with all the other assessment modalities and to be used effectively in diagnosis, prognosis and treatment.

1.1 BASIC CONSTRUCTS

We consider the development and evolution of diagnostic imaging. This is outlined below for an example in ultrasound scanning of the thyroid.

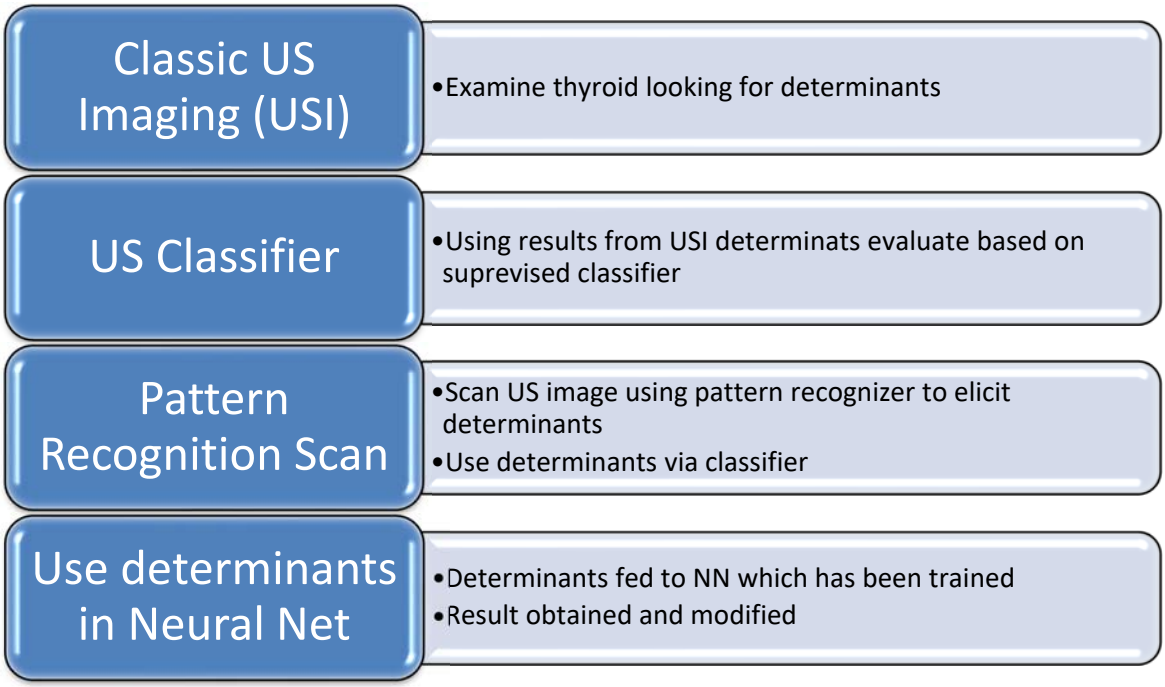

The classic baseline is a manual scan with interpretation of the scan by a radiologist. The radiologist examines the scan in the three dimensions across multiple regions looking for possible nodules and in turn looking for specific characteristics of those nodules. A normal thyroid is devoid of such nodules but as the patient ages nodules become quite common. The nature of the nodule such as hypoechoic, solid, containing microcalcifications are often indicative of a malignant state. The radiologist looks for these visually and places these observations in their report.

A second stage in the development is the inclusion of the observations into a classifier. Namely taking the measurements or just presence of some characteristic into an algorithm would could provide diagnostic implications would take the analysis to a second step.

A third step is to aid the radiologist by digitally recognizing patterns such as a solid nodule, a hypoechoic nodule or a microcalcification. The image recognition process enhances the

radiologist's ability to minimize missed lesions. The image recognition process looks for the characteristics generally a priori considered indicative.

A fourth step would be the implementation of a deep learning or neural network approach, wherein using some supervised system of training between benign and malignant tissues, scan are made of the ultrasound and processed by the neural net based upon volumes of trained results and the net then determines the presence or absence of a malignancy.

Clearly the fourth step deletes the need for a radiologist.

1.2 SOME STATISTICS

We preface the study with two examples. Both are somewhat simplistic but in use. First is the analog example, namely one where we make measurements of factors which are variable numbers. The second is digital, namely a case where something is or is not. This characterization is somewhat unique but it seems to apply to a wide variety of cases. In addition the first case is based upon measurements of bodily fluids and other quantitative measures and the second on images which either present a characteristic or not.

1.2.1 Analog Variables

Let us begin with some basic definitions. Recall that:

$$Sensitivity = P\left[H_1 \middle| H_1 \right]$$
$$Specificity = P\left[H_0 \middle| H_0 \right]$$

Sensitivity is the probability of saying a person who has the disease has the disease based upon the test.

Specificity is the probability that a person who does NOT have the disease is said to NOT have the disease based upon the test.

The sensitivity and specificity depends upon the variability of the metric used to test for the presence or absence of the disease and well as the check point or marker for the metric which yields presence or absence of the disease.

Let us look at a simple example. Let us assume we have a test for prostate cancer which depends upon:

1. PSA
2. % Free PSA
3. Velocity
4. Age
5. Family history

6. Prior most recent biopsy history (benign, BPH, HGPIN)

We can measure these. Then we create some metric:

$$m = f(x_1, ..., x_6)$$

or

$$m = \sum_{i=1}^{6} a_i x_i$$

The metric m is a classifier metric and the linear version is a linear classifier. Now a modified version could be:

$$m = \sum_{i=1}^{6} a_i g(x_i)$$

where we choose the g functions to give a better performance. For example one may use a logistic function of the like where there is some one-to-one mapping. This is a quasi linear classifier.

Now if we choose some point p, where if m>p we declare a PCa and m<p then no PCa we have a classifier. Now each value of p would yield a different sensitivity and specificity. If we were to plot Sensitivity versus 1-Specificity, namely the probability we say a disease when there is a disease versus the probability we say there is a disease when there is no disease we get a curve whose area we can calculate. Hopefully we can say there is a disease when there is with high probability and that we say with low probability that there is a disease when there is none. This can be measured by the area under this curve, AUC.

1.2.2 Digital Variables

Let us now consider an example. Here are measurements for thyroid ultrasound tests. We have:

Characteristic Present or Absent	*Sensitivity PRESENT Say disease when has disease*	*Specificity ABSENT Say no disease when no disease*
Hypoechoic c/w (consistent with) surrounding thyroid	81% (48-90%)	53% (36-92%)
Marked hypoechogenicity c/w strap muscle	41% (27-59%)	94% (92-94%)
Microcalcifications	44% (26-73%)	89% (69-98%)
Macrocalcifications	10% (2-17%)	94% (84-98%)
Absence of halo	66% (33-100%)	43% (30-77%)
Irregular, microlobulated margins	55% (17-84%)	80% (62-85%)
Solid consistency	86% (78-91%)	48% (30-58%)
Taller-than-wide shape on transverse view	48% (33-84%)	92% (82-93%)

In the table we see that a solid consistency of a nodule has an 88% sensitivity but a 48% specificity. Thus a solid nodule means that there is a high chance of saying malignant when it really is. In contrast we are about 50:50 saying it is not when it is not. In contrast with no macrocalcifications we have a 94% chance of saying it is not when it is not but the presence of them may be only a 10% that there is when there is. Now the range of the values is also critical and we shall examine that in a bit.

All of the metrics above are binary. Namely the characteristic is present or not. This is unlike the PCa example of a real number. There are 8 metrics where we have a present or absent. The question then is:

Can we improve the AUC by using a classifier which in some manner combines all eight elements? If so, how should they be combined and weighted?

Thus we can ask; what is we have four characteristics being positive? What then is the specificity, the sensitivity? What is also the other four are negative? Does it matter greatly what four and four we are talking about?

Let us consider another question. Let us assume we do not read this with a human but by a computer. Consider hypoechoicity and microcalcifications. We can develop a pattern recognition system to identify each of these, the first via a system looking for expansive hypoechoic areas and second by looking for hyper stellate patterns of a certain size range.

Now we can ask the following question. How does the sensitivity and specificity change as we add multiple measures? Specifically, as mentioned above, considering hypoechoic with microcalcification, two elements which are either present or not, each having a certain level of performance, what happens to our metrics when we use both?

We know:

$$P\left[Cancer\middle|Hypoechoic\right]=\alpha$$

and

$$P\left[Cancer\middle|Microcalcified\right]=\beta$$

thus

$$P\left[Cancer\middle|Hypoechoic,Microcalcified\right]=\gamma$$

Thus, what is the value of the third expression given the first two. More importantly just what is meant by the latter expression. We can have the following:

$$P\left[Cancer\middle|Calcified,Hypoechoic\right]=$$

means having calcification and hypoechoic

or

having calcification and hypoechoic

This we can consider it as follows graphically. Here we show a region where the cells are malignant and those where they are not. The circles represent a region where a certain characteristic is observed. The intersection of the characteristic and the malignancy is the measure of saying a malignancy given a characteristic when a malignancy exists. Or equivalently the percent of the circle in the malignant area is a measure of the probability of a malignancy when a characteristic exists given a malignancy exists. Thus we can show it below:

P[Cancer|Calcified, Hypoechoic]=P[Cancer|Hypoechoic]+P[Cancer|Calcified]-Overlap

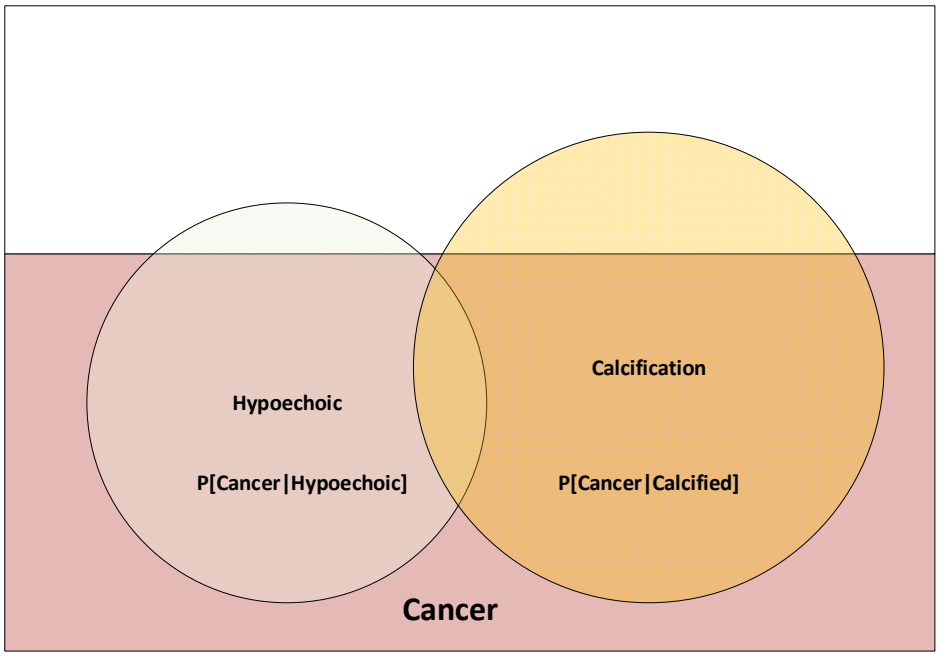

or as the probabilities expand:

P[Cancer|Calcified, Hypoechoic]=P[Cancer|Hypoechoic]+P[Cancer|Calcified]-Overlap

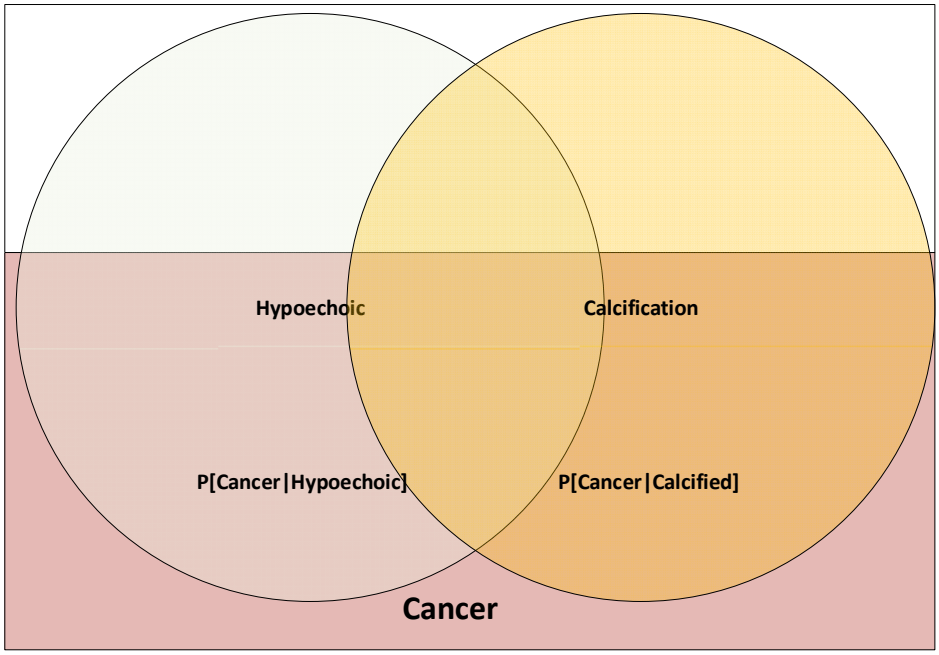

Note if we assume the or, it is then the probability of both less the overlap, whereas if we assume both then it is just the overlap. The or case yields a greater sensitivity whereas the and case is lesser. As we add all eight factors we can determine the AND the OR cases. The OR cases ultimately converge to 1.

Namely we can write:

$$P\left[Malignant \middle| Hypo\ or\ Calci\right] = P\left[M \middle| H\ or\ C\right] =$$
$$P\left[M \middle| H\right] + P\left[M \middle| C\right] - P\left[M \middle| H\ and\ C\right]$$
but
$$P\left[M \middle| H\ and\ C\right] = P\left[M \middle| H\right] P\left[H \middle| C\right]$$

Clearly, we do not have the data on the last conditional probability of H given C. This is the probability that H is true given C is true. Expansion to all eight terms should be obvious. Namely:

$$P\left[M \middle| x_1, or ... or, x_n\right] =$$
$$\sum_{i=1}^{n} P\left[M \middle| x_i\right] - \sum_{i=1}^{n} \sum_{j=1}^{n} P\left[M \middle| x_i\right] P\left[x_i \middle| x_j\right]_{i \neq j} - multiples$$

We show an example of the multiples below where we have the intersection of all three conditions.

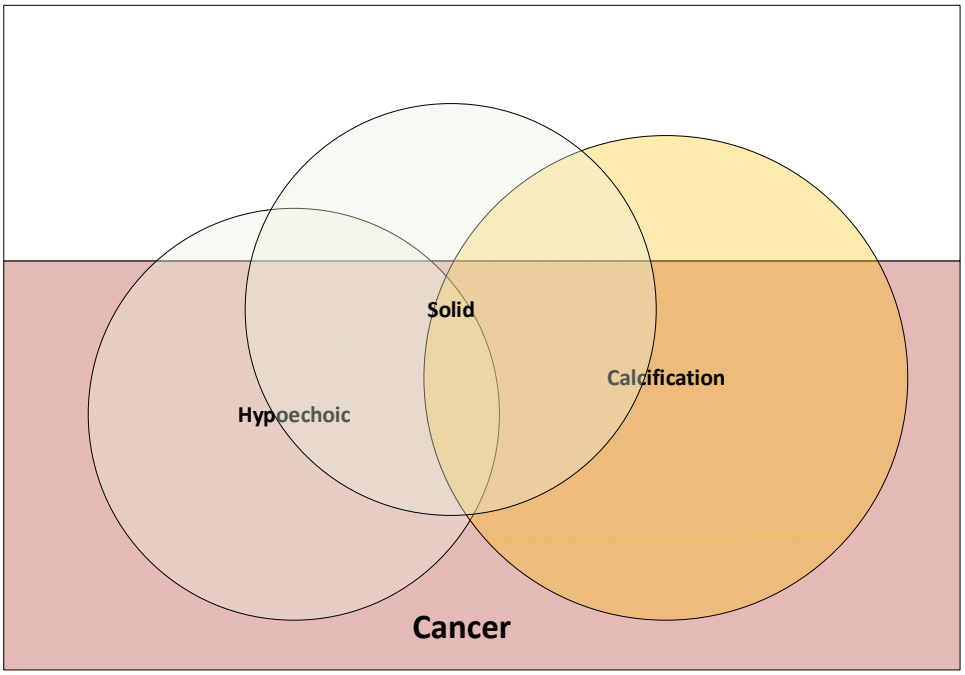

The model here is:

$$P\left[Malignant\left|Hypo\ or\ Calci\ \text{or}\ Solid\right.\right]=P\left[M\left|H\ or\ C\ \text{or}\ S\right.\right]=$$
$$P\left[M\left|H\right.\right]+P\left[M\left|C\right.\right]+P\left[M\left|S\right.\right]$$
$$-P\left[M\left|H\ and\ C\right.\right]-P\left[M\left|H\ and\ S\right.\right]-P\left[M\left|S\ and\ C\right.\right]$$
$$-P\left[M\left|H\ and\ C\ \text{and}\ S\right.\right]$$

but

$$P\left[M\left|H\ and\ C\right.\right]=P\left[M\left|H\right.\right]P\left[H\left|C\right.\right]$$

etc

or

$$P\left[Malignant\left|Hypo\ or\ Calci\right.\right]=P\left[M\left|H\ or\ C\right.\right]=$$
$$P\left[M\left|H\right.\right]+P\left[M\left|C\right.\right]-P\left[M\left|H\ and\ C\right.\right]$$

but

$$P\left[M\left|H\ and\ C\right.\right]=P\left[M\left|H\right.\right]P\left[H\left|C\right.\right]$$

yet

$$P\left[M\left|H\right.\right]P\left[H\left|C\right.\right]=P\left[M\left|C\right.\right]P\left[C\left|H\right.\right]$$

thus

$$\frac{P\left[M\left|H\right.\right]}{P\left[M\left|C\right.\right]}=\frac{P\left[C\left|H\right.\right]}{P\left[H\left|C\right.\right]}$$

also

$$P\left[M\left|H\right.\right]+P\left[M\left|C\right.\right]-P\left[M\left|H\right.\right]P\left[H\left|C\right.\right]=$$
$$P\left[M\left|H\right.\right]\left(1-P\left[H\left|C\right.\right]\right)+P\left[M\left|C\right.\right]\le 1$$

or

$$\frac{P\left[M\left|H\right.\right]+P\left[M\left|C\right.\right]-1}{P\left[M\left|H\right.\right]}\le P\left[H\left|C\right.\right]$$

We shall discuss these implications later. However several observations are important. The probabilities such as P[H|C] are generally unknown. Namely the relationship between disparate indicators. Thus PSA and %Free may be independent or highly dependent. Studies have not indicated specifically and the underlying cellular dynamics, albeit somewhat understood, may not be complete.

This means that as we look at specifics which we can measure that they may be correlated and as such we must understand those correlations both factually as well as physiologically.

1.3 SUMMARY

Thus we will now summarize our approach.

First we review the current variety of imaging modalities, from classic radiology, thru ultrasound, and including cytology and histology. The intent is to focus on the images which are created in the context where they can be analyzed using current computer methods.

Second, we spend some time on mpMRI, multi parameter MRI, as a robust imaging technology. In this case we examine the multiplicity of ways the images can be analyzed from classic human interpretation through convolutional neural nets. This introduces the issue of image analyses using two-dimensional image operations.

Third, we briefly discuss the elements of genomics. Frankly there must be a well-defined nexus between the genomics and the Eikonomics analyses. Unfortunately they currently are orthogonal to each other, each bringing separate inferences in diagnosis.

Fourth we examine several different malignancies to evoke the Eikonomics of each.

Overall this document is not meant to be an encyclopedic presentation of various forms of imaging and their integration. Rather it is at best an exploratory statement of what may be a variety of open options to explore images in an integrated manner and to do so at various levels of automated sophistication. The reader may notice a certain hesitancy regarding the unbounded use of neural networks. The reason is simple. The principle of training a complex neural network totally in the hands of the network qua arbiter of inputs, facilitates the total loss of underlying facts. First we know that neural network designs do not necessarily converge to a common answer. Second, medicine often is solved by some pathognomonic set of symbols and signs.

As Stoyanova et al have noted, the progression can be viewed as shown below:

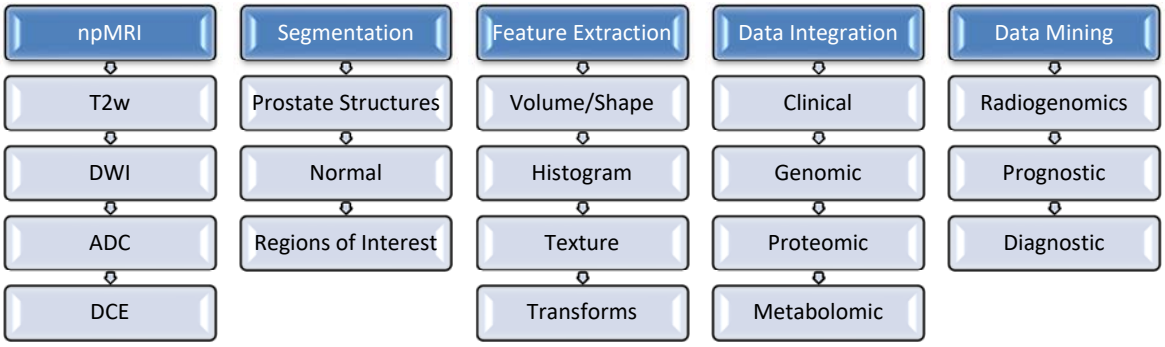

The above progression is at the heart of what we are calling Eikonomics.

2 IMAGING

We briefly examine the multiplicity of imaging modalities. This is in no way complete but it is representative. As we noted earlier, we focus on images from which we can ascertain diagnostic and prognostic metrics. Images, unlike say PSA, are much more complex and contain a higher degree of information. The increase in information may be beneficial but it also may find itself as a distraction. For example if we are looking for solid lesions or calcifications in a thyroid ultrasound, then the multiplicity of other factors may be mere noise to that ultimate decision process. The human can be trained to filter out the noise, the machine must "learn" how to accomplish that.

2.1 US

Ultrasound, US, is a real time imaging tool which can measure a variety of characteristics. It is limited by the depth of penetration from the sensor to the target tissue. It serves a variety of uses from breast, prostate, thyroid, heart and other organs. The thyroid application is quite demonstrative of what it can accomplish and the prostate use during biopsy now functions with mpMRI.

US has its limitations. It demands proximity to the tissues being investigated. It has limited resolution, since the wavelength of the sound even at 15 MHz is not that great. It can assess general tissue structure, solid versus cystic, the presence of such things as calcium crystals, if large enough, and using doppler the flow through the tissues. It can work on thyroids, breast, ovaries, prostate, even the heart. It can do vascular assessments. It can lend some substance to possible malignancies but it is not dispositive.

From Wang et al (2019):

Categories	Description	Methods
Texture	Reflects the surface characteristics of a lesion and it is frequently used in traditional CAD system.	• Laws Texture Energy (LTE) • Contrast of Gray Level Values • Gray Level Cooccurrence Matrix (GLCM) • Local Binary Pattern (LBP) • Wavelet Features
Morphology	More focus on lesion itself. Such as smoothness of lesion margin, length and width ratio of lesion and so on	• Speculation • Depth-to-Width Ration • Elliptic-Normalized Circumference (ENC) • Elliptic-Normalized Skeleton (ENS) • Long Axis-to-Short Axis Ratio (L:S)
Model Based	Statistical model of the backscattered echo that can indicates the character of backscattered echo from tissues.	• Nakagami model-based features • K-Distribution model-based features
Descriptor Features	Different applications (diseases) create different descriptor features and features are generated by radiologist base on their experience	• Shape • Calcifications • Posterior shadow or posterior echo • Echo characteristic

Also from Wang et al (2019) as modified:

Classifier	Description
Linear Classifier	Linear discrimination analysis and logistic regression are two linear classifiers and reliable only with linear data.
Bayesian Classifier	It is involved in machine learning and it predicts posterior information base on analyzing previous data points.
Support Vector Machine	Kernel functions are utilized to find decision hyperplanes by computing the original data into the higher dimensional space. The complexity increases as dataset increases.
Decision Tree	Its structure is a flowchart and it computes classification rules from disordered data. The size of data and feature values affect the complexity of the decision structure.
Artificial Neural Network	It is a machine learning model base on human nervine system. The complexity of the network affects the training time.
AdaBoost	Integrating several weak classifiers and building a strong classifier based on prediction voting from weak classifiers.

2.2 CAT

CAT is a classic form of ionizing radiation used to reconstruct in a 2D and 3D manner the tissues in the path of the beam. It is an example of what is called the inversion problem, a method of taking a multiplicity of paths and their total signal response and then interpolating what the transmission was at each pixel along the path. The basic principle of the CAT is the use of the Radon transform and its relationship to the Fourier transform. Having been used clinically in the

US since 1972 it is a relatively inexpensive and fast screening tool, albeit putatively highly ionizing.

We shall see that it has use in certain screening of malignancies such as colon cancer. Contrast media may also be employed and this may increase the usefulness of this methodology.

2.3 MRI

MRI is a powerful soft tissue imaging modality and it has a great deal of flexibility in its abilities by selectively choosing various activation pulses. Basically MRI operates by placing the tissue in a strong magnetic field, displacing the field, and measuring the resulting signal. Using the inverse Fourier transform we can determine the tissue characteristics across each scan, and constructing them in the three dimensional slices. In a sense MRI is more powerful than CAT especially on soft tissues however is it more costly and does have certain negative patient reactions.

2.4 2D, 3D, OR 4D IMAGING

Many if not most imaging studies are 2D. They may be slices of coronal, sagittal or transverse cuts. The objective is to scan the target area for abnormalities observable on the imaging modality.

3D imaging has been used in neuro environment and certain cardio environments as well.

4D imaging is 3D with a temporal element, Again in a cardio environment such as valve abnormalities this may have application.

2.5 CYTOLOGY AND HISTOLOGY

Cytology, the cell analysis, and histology, the micro-structure analysis, are also two branches of imaging which can be considered. Thus a cytological exam could entail looking at thyroid cells where the issue is the structure of the nucleus and nucleolus, even the nature and form of the cell and nucleus walls. In contrast the histological examination of the prostate may look for basal and luminal cell organization and proliferation. Imaging in a general sense, here we are using visual albeit microscopic images, can be helpful in diagnosis and prognosis. Many of the techniques in other imaging fields apply here as well.

Histological analysis can provide an understanding of the tissue structures, the assembly and organization of cells in the tissue in question. Thus we can examine a prostate biopsy specimen and see if it has the cellular amalgamation that may be reflective of HGPIN or even PCa. In a similar manner we can examine the structure of a skin biopsy to see if the melanocytes have migrated upward and we have a melanoma in situ or worse if they have migrated downward into large clusters.

From Brinster et al we have an example of a superficial spreading melanoma[1].

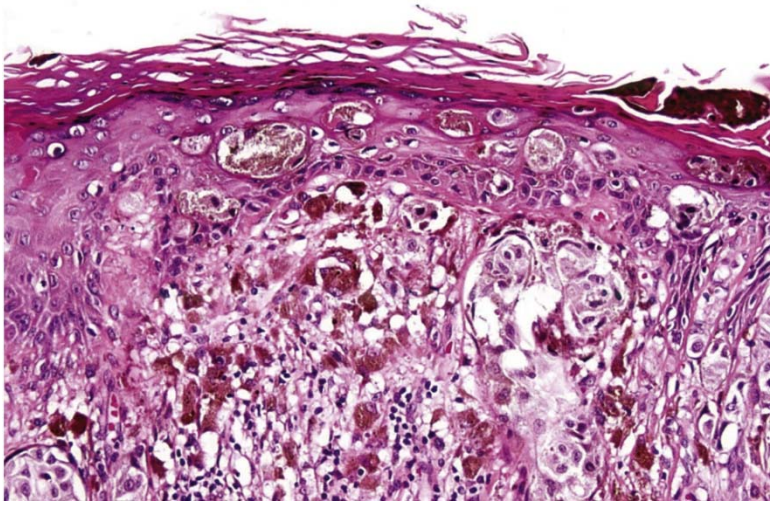

In contrast we have from Su et al[2] a presentation of various forms of prostate HGPIN:

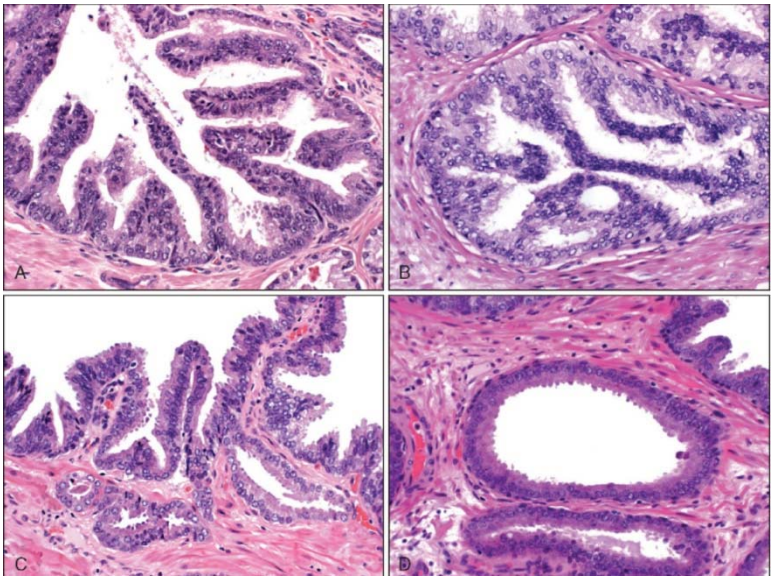

As we focus on images we can see that identifying a malignancy or possible malignancy automatically can be quite complex. The pathologist looks for telltale forms, clusters of

[1] Brinster et al, Dermatopathology, Saunders, 2011

[2] Su et al, Early Diagnosis and Treatment of Cancer: Prostate Cancer, Saunders, 2010

melanocytes as in the melanoma example or proliferation of prostate cells in a less organized form as in HGPIN.

Now cytological metrics, namely single cell characteristics, also play a role. For example, consider thyroid cancer, papillary characteristics.

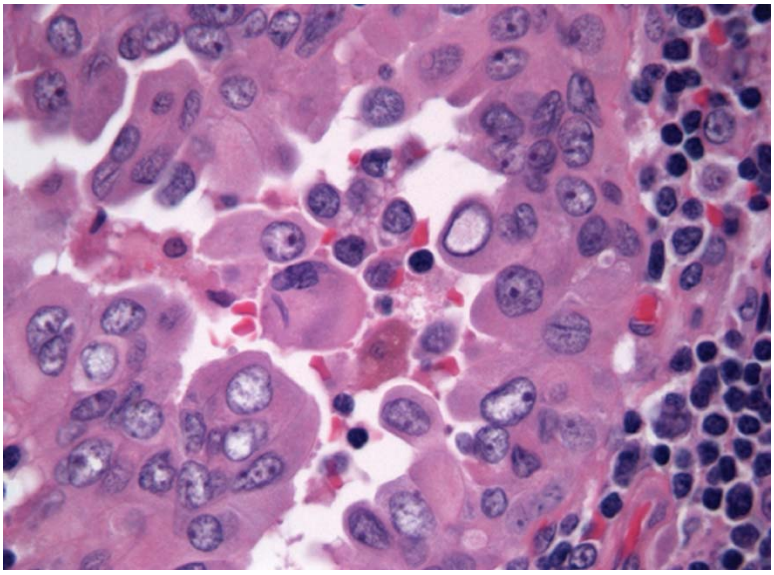

Here we have an example of papillary cancer with clear nuclei[3]. Thus searching at the cell level in this malignancy allows for a diagnosis. There also are histological clues as well.

[3] Boerner, Biopsy Interpretation of the Thyroid, Wolters Kluwer, 2017

3 mpMRI OPTIONS: IMAGE ANALYSES

We now spend some time examining mpMRI image analyses. What we consider here can in many ways be applied to the other image modalities discussed. mpMRI is a complex utilization of various MRI modalities. It uses T1 and T2, as well as diffusion weighted MRI and dynamic contrast enhanced MRI. Thus using the ability to have a T1 and T2 signal, allow enhancement of various tissues, using diffusion as a means to identify benign from malignant and in the use of contrast such as gadolinium, one can obtain a set of overlaid images that enable a deeper understanding of the prostate tissue as an example. We now will attempt to examine how this set of complex issues can then be further employed with US imaging or other forms in identifying a putative malignancy.

mpMRI is basically a three-process approach.

First is the use of T2 weighted images. These are now standard imaging.

Second is diffusion weighted images, DWI, and these attempt to assess the flow through cell masses. Health cells allow flow or diffusion and cancer cells inhibit. Unfortunately so do scar tissues from previous biopsies. Thus as in all of these methodologies there may be drawbacks.

Third is DCE or dynamic contrast enhancements, which use a contrast medium such as gadolinium and dynamically asses its flow to determine vascular structure.

Thus, mpMRI is T2, DWI and DCE. From these three we get a full mpMRI analysis[4]. The mpMRI results are structure, density, and vascularization. When we use this approach we can see parts of the organ that may be of interest, assess whether the cells are original or replacements, and if the region has any increase in vascularization or growth. That then yields information which can be used to assess malignancy potential.

3.1 GENERAL ASSUMPTIONS

We will start with an understanding of a simple statistical construct. Let us assume there are N variables which can be measured to determine if a person has a certain disease state. We then can determine:

$$P\left[Disease_k \mid x_n\right] = p_{k,n}$$

Namely we know by data the fact that given the n state we can determine a specific disease state k.

We also have:

$$q_{k,n} = 1 - p_{k,n}$$

Now lest us assume that we have N of the measurements. Let us examine a simple 2 measurement example with two disease states.

$$P\left[D_1 \mid x_1, x_2\right] = P\left[D_1 \mid x_1, x_2\right]$$

Let us focus on mpMRI as a start. The question we pose is; what do we mean by radiomics using mpMRI? For example, is it totally computerized or totally reliant upon the radiologist? Do we send the patient into the imaging system and out comes a diagnosis? Or do we image a patient and have the radiologist make all the judgements? How much and how far do we allow the system to function?

For example, in breast mammography we generally perform an x-ray study and then the radiologist examines the image looking for signs of a malignancy. They are generally two-dimensional films, now electronic,

3.2 GENERALIZED METRICS

The classic approach is in line with RECIST protocols used in clinical trials. As Eisenhauer et al have noted describing RECIST:

Assessment of the change in tumour burden is an important feature of the clinical evaluation of cancer therapeutics. Both tumour shrinkage (objective response) and time to the development of disease progression are important endpoints in cancer clinical trials. The use of tumour regression as the endpoint for phase II trials screening new agents for evidence of anti-tumour effect is supported by years of evidence suggesting that, for many solid tumours, agents which produce tumour shrinkage in a proportion of patients have a reasonable (albeit imperfect) chance of subsequently demonstrating an improvement in overall survival or other time to event measures in randomized phase III studies.

At the current time objective response carries with it a body of evidence greater than for any other biomarker supporting its utility as a measure of promising treatment effect in phase II screening trials. Furthermore, at both the phase II and phase III stage of drug development, clinical trials in advanced disease settings are increasingly utilizing time to progression (or progression-free survival) as an endpoint upon which efficacy conclusions are drawn, which is also based on anatomical measurement of tumour size.

3.3 CLUSTER ANALYSES

Cluster analysis is a now classic means to group data into classes. One may have supervised or unsupervised and there are a variety of clustering algorithms such as nearest neighbor clustering. Generally we will not use clustering here.

3.4 PATTERN RECOGNITION

Pattern recognition has been available in one form or another for decades. It has been used in a wide set of areas. Pattern recognition techniques allow for the "extraction" of key patterns to be used in discrimination. Thus using edge extraction in modifying say a US image we can then look for a pattern representative of a papilla like growth. We can look for pedunculated lesions, look for cyst like surfaces or look for clear nucleus or Orphan Annie eyes. Pattern recognition tools allow for the extraction of know or unknown patterns. If for example we know that certain patterns are pathognomonic then we can design a pattern recognition system to look for those specific patterns.

We believe that the development of pattern recognition and extraction methods will be at the heart of any successful classification scheme. The patterns will produce metrics which we can then use in the classification.

3.5 CLASSIFICATIONS; SUPERVISED AND UNSUPERVISED

Classifiers take multidimensional data sets and establish lines of demarcation separating one class from another. The example of using PSA and %Free and seeking the dividing line between benign and malignant allows for a reasonable test. Multidimensional classifiers are much more highly structured.

We can now measure various miRNAs in body fluids and this gives rise to the liquid biopsy concept. However, the key question is how does one take a collection of miRNA measurements and ascertain, for example, that there is a prostate malignancy. For example we may from the previous presentation generate a vector of measurement of miRNA densities given by:

$$m_k = \begin{bmatrix} x_1 \\ \dots \\ x_n \end{bmatrix}$$

where this is for patient k and measures n miRNA densities. We want a discriminant function which takes these values and determines whether the patient has cancer of not. We could have a linear weighted discriminant or a more complex non-linear version.

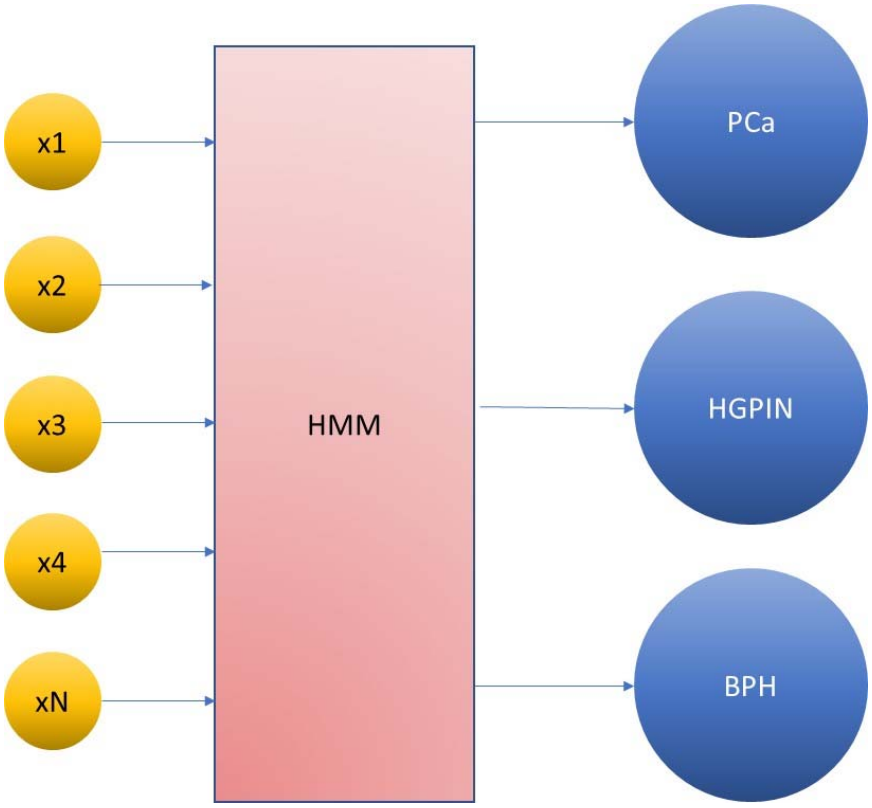

We can look at a Markov model as below. However these transition probabilities are often difficult to determine.

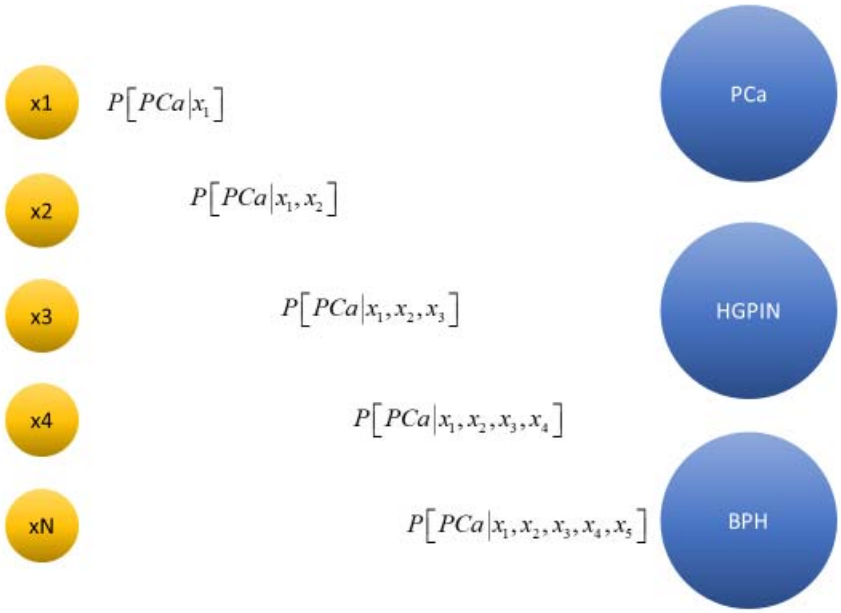

$$P[x_1|PCa]$$
....
$$P[x_1,...,x_N|PCa]$$
or
$$P[PCa|x_1]$$
....
$$P[PCa|x_1,...,x_N]$$

where we have the two probabilistic ways to ascertain a condition based upon a data set.

Let us consider a simple example. Assume we have to determine if a patient has prostate cancer or not. We are given three variables; PSA, % Free PSA, and PSA velocity[5]. Namely:

PSA=PSA

[5] See: Carter et al, Detection of Life-Threatening Prostate Cancer With Prostate-Specific Antigen Velocity During a Window of Curability, Journal NCI Vol 98 Nov 2006 pp 1521-1527, https://academic.oup.com/jnci/article/98/21/1521/2521858

PF=% Free PSA

V=PSA Velocity

Thus we have three measurements and they are somewhat related. Let us start with two of them; PSA and PF. The data may appear as shown below:

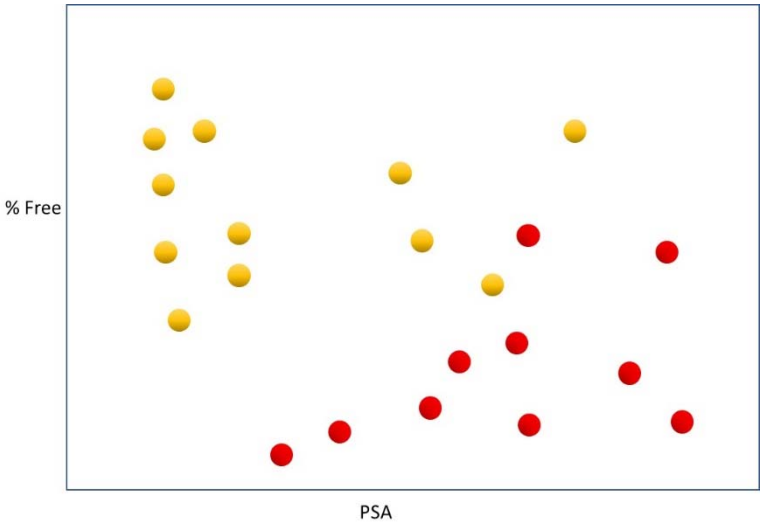

The red are PCa cells and the orange are benign. The higher the PSA the greater the chance for PCa. However, the higher the PF the greater the chance for benign, namely BPH. This is a simple case where we would have some discriminant where both variables count.

Now consider all three variables. We have PSA, PF and V. We need a discriminant so as to separate malignant from benign. We have data ex post facto so this is a supervised learning algorithm. We need to obtain some covering surface that maximizes the sensitivity and specificity. The algorithm must maximize the AUC. The more data the better the algorithm, yet we will always have aberrant cases.

The challenge in this case is that the discriminant is not a simple plane of some sort. It can be a complex surface winding its way around the 3-space. Namely the 2-space example shown in the above diagram may change for every V measure. For any V value we can obtain a 2-space profile. But that profile is different for every V and each has a different AUC. We can design a simple process where we enter all the data and calculate that surface on a cut by cut basis. Then any user can enter the three variable and get a result; benign/malignant, specificity, sensitivity.

Now let us consider a simple linear discriminant for PSA/PF and for a fixed V. Our goal is to select a curve:

$$PF = aPSA + PF_0$$

The goal is to obtain "a" and PF_0 so that we maximize both sensitivity and specificity. This can be readily accomplished by a variety of simple algorithms.

The next question would be; how many data points do we need and how frequently must they be updated? The answer can really only be obtained in an iterative manner with real data. We know that PSA alone has at best an AUC of 70%. Obtaining the AUC in this three element case is more complex. We may also want to add such elements as age, family history, prior biopsy results and the like. Each element adds another layer of complexity.

A simple and direct approach would be a linear classifier. Our metric is sensitivity and specificity. Namely:

$$Sensitivity = P\left[H_1 \middle| H_1 \right]$$

and

$$Specficity = P\left[H_0 \middle| H_0 \right]$$

If the discriminant plane is:

$$g(x) = ax + b$$

where

$$x = \begin{bmatrix} x_1 \\ \dots \\ x_N \end{bmatrix}$$

$$a = \left[a_1 \dots\dots\dots a_N \right]$$

The goal is given the data set, find the **a** vector and b to separate the data so as to maximize sensitivity and specificity[6].

There are a multiple set of classifiers and our selection of a linear classifier in a supervised environment is just one of many. We do not know the underlying statistics of the miRNA and also each miRNA itself may or may not be as strong an element in classification. Some miRNA that we choose may be a weak element and should be eliminated. That can only be ascertained after extensive data analysis.

Another way one could examine this partition problem is to assume that the two variables we discussed earlier, say PSA and PF, are independent Gaussian variable with mean and standard deviations:

[6] We refer to Theodoridis and Koutroumbas and their work on classification. We note that there are a multiplicity of algorithms to define this linear classifier. Also, there is a great deal on PCa learning algorithms in Hastie et al.

H_0 :

$m = m_0, \sigma = \sigma_0$

H_1 :

$m = m_1, \sigma = \sigma_1$

Then we could use classic decision analytical methods to determine optimal selection criteria. We could estimate the mean and variance from the given data and even ascertain a probability density function to see if it varies from Gaussian. It is not clear that such an approach yields better discrimination.

Finally, one could seek to use a Principal Component Analysis to determine optimal orthogonal axes[7]. However, again in my experience, this would not gain a great deal.

A linear classifier using the large data set may be more than adequate. We show below several examples of a linear classifier for PSA vs FP[8].

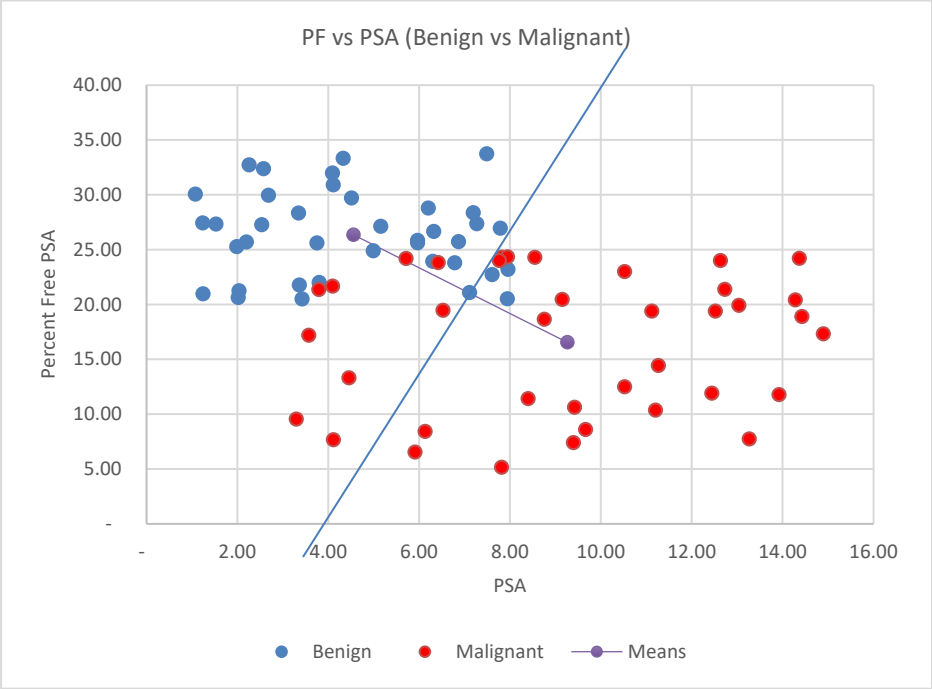

and for a second dimension we depict this below:

[7] See Dunteman, Principal Component Analysis, Sage University Paper, 1989.

[8] We use the reference of Duda and Hart, Pattern Classification, 1st Ed, Wiley, 1973.

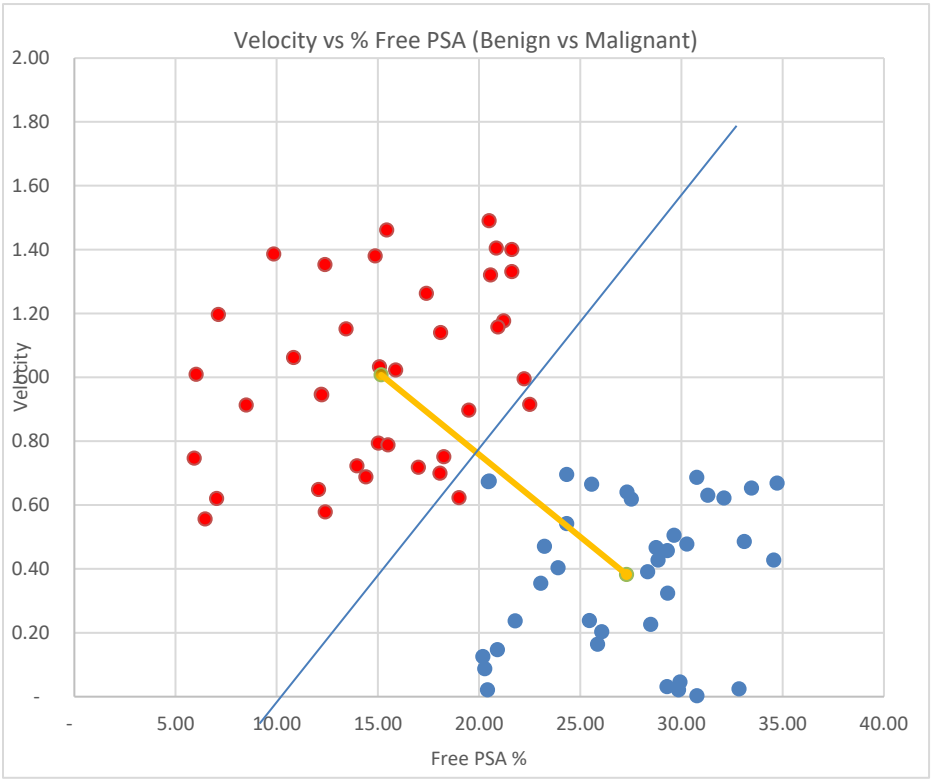

Note all have different data yet all have same means on the two data sets. Thus the slope of the classifier is the same and intercept changes a bit. This same approach carries over to the miRNA context for multiple dimensions.

Now classifiers can often be nonlinear. The above simple example assumed a linear deign. However better performance may be obtained with a nonlinear classification scheme. The simplicity of the above classifier is based upon two facts. First, we know from the data who is benign and who is malignant. Second, we have selected elements, three in this case, upon which we can segment and classify.

In our study of images we do not necessarily have elements to be used to establish a classification. We start with a set of digital images. Perhaps from the images we can obtain a finite set of metrics, perhaps not. The next discussion is on neural networks, a more sophisticated from of classifier.

3.6 NEURAL NETS

Imaging analysis using neural networks often uses a convolutional neural network. The input may be an N X M matrix of k bit pixels. Namely a digital picture. We then collect are large set of such pictures and using knowledge of the disease state a priori we pass them through a network whose weights of connections are adaptively changed so as to maximize the probability that if we put in an unknown we get a very good guess as to whether it is benign or malignant.

In such a design we often use a convolution processor which passes on to the next layer a new meta-pixel which can be some integration or enhancement of the basic input. We show this construct below.

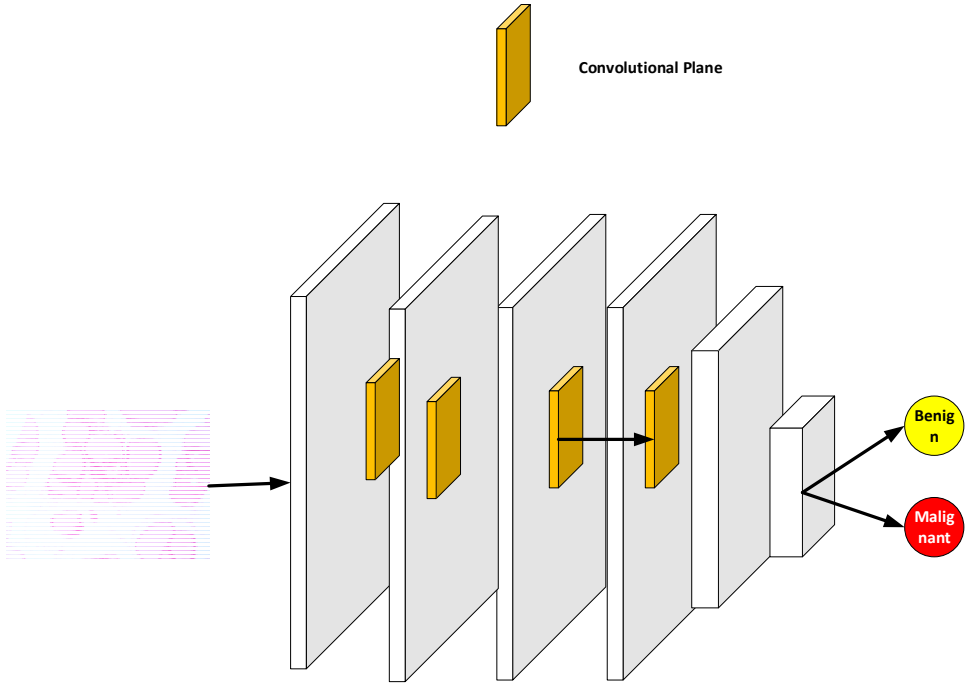

It functions as follows:

1. A two dimensional image, properly sized, is samples into a two dimensional input plane in the network. It is identified as benign or malignant, and that is all.

2. The network has n planes and each plane has a convolutional filter as noted. Thus the entry on the following plane is comprised of (k x k) convolved samples of a segment of the prior plane.

3. A backward propagation algorithm is used as the network is trained. Namely M samples, each identified as malignant of benign, is passed through the network and the weights between layers are modified to optimize the output based on the known sample. Classically this may have been a least squares algorithm as was done in the classic Widrow Hoff optimizer for phased array antenna beam forming[9].

4. After the M samples are used to set the weights, the unknown is entered and the sample unknown identified.

Needless to say there are several key differences:

[9] See Monzingo and Miller, Introduction to Adaptive Arrays, Wiley, 1980, Chpts 3-4, VanTrees, Optimum Array Processing, Wiley, 2000.

1. No a priori patterns are selected. In fact, the network does not even assume that there are cells there. It has been trained on a large number of patterns.

2. The user may have no idea what the patterns emphasis may have been. Thus after some training period, the user is relying on the network to select what is a discriminant and what weight it may have.

The algorithm for neural networks with training is generally simple to grasp but it has many variations. Namely, data sets x consisting of say n x n arrays of 8 bit grey scale samples are used to put into a single hidden neural net, where we have say an m x m array of weights a which we want to train to discriminate between a disease state. The algorithms generally look like:

$$a = \begin{bmatrix} a_1 \\ \dots \\ a_m \end{bmatrix}$$

and

$$x = \begin{bmatrix} x_1 \\ \dots \\ x_N \end{bmatrix}$$

where

$$\hat{a}(k+1) = \hat{a}(k) - K(\hat{a}^T(k)x(k) - s)$$

where K is some convergence matrix. Namely we train the neural net with a massive number of samples whose sate "s", the disease, we know, and generate a(k), to reach some stable state, hopefully. Then with an unknown we send it into the net and hopefully get the correct disease state.

Now a brief overview of the Least Square Estimate procedures. Let us assume we are trying to estimate the slop and intercept of a straight line:

$$y = ax + b$$

we have N sets of x and y values, all somewhat noisy. That is:

$$x = \begin{bmatrix} x_1 \\ \dots \\ x_N \end{bmatrix}$$

and

$$y = \begin{bmatrix} y_1 \\ \dots \\ y_N \end{bmatrix}$$

Now we want a recursive estimator of the form (as we note to be a least square steepest descent model):

$$\hat{a}(k+1) = \hat{a}(k) + \Delta_a(y(k) - \hat{a}(k)x(k) - \hat{b}(k))$$

and

$$\hat{b}(k+1) = \hat{b}(k) + \Delta_b(y(k) - \hat{a}(k)x(k) - \hat{b}(k))$$

This is based on steepest descent algorithms and the choice of the function for the descent is based upon a least square performance function[10]. Namely we want to minimize:

$$\varepsilon^2 = \left[y(k) - \hat{a}(k)x(k) - \hat{b}(k) \right]^2$$

Classic least square has the descent function be that which minimizes the error for each element being minimized. Namely:

$$\frac{\partial \varepsilon^2}{\partial \hat{a}(k)} = \frac{\partial}{\partial \hat{a}(k)} \left[\left[y(k) - \hat{a}(k)x(k) - \hat{b}(k) \right]^2 \right]$$
$$= 2\left[y(k) - \hat{a}(k)x(k) - \hat{b}(k) \right]$$

and the same for b. Thus, the steepest descent for a least square estimator is as we have shown above. The constants are chosen for convergence purposes and they are negative.

Now in a complex neural network we take the image which may be two dimensional and use each pixel as an input. Then we may convolve the image in some manner with a small m x m filter and pass it along. The weights at each step are adaptively changed if say a supervised test is performed. The neural net weights change in a manner similar to the linear estimator discussed above. We incrementally change them as we send identified image after image into the system[11].

[10] See Athans et al, Systems, Networks, and Computation, McGraw Hill, 1974

[11] See Hakim

There are now a massive number of algorithms to be used and with multiple layers as shown below we have deeper and deeper nets. Again the issue is that we are relying on the net to identify the diagnostic issues and we may never know what the net sees as important.

Now an added approach is to establish a pattern recognition front end where we can identify such things as edges, MDI artifacts, cell size, cell counts and the like. Then we feed those parameters to the Neural Net. We show this below.

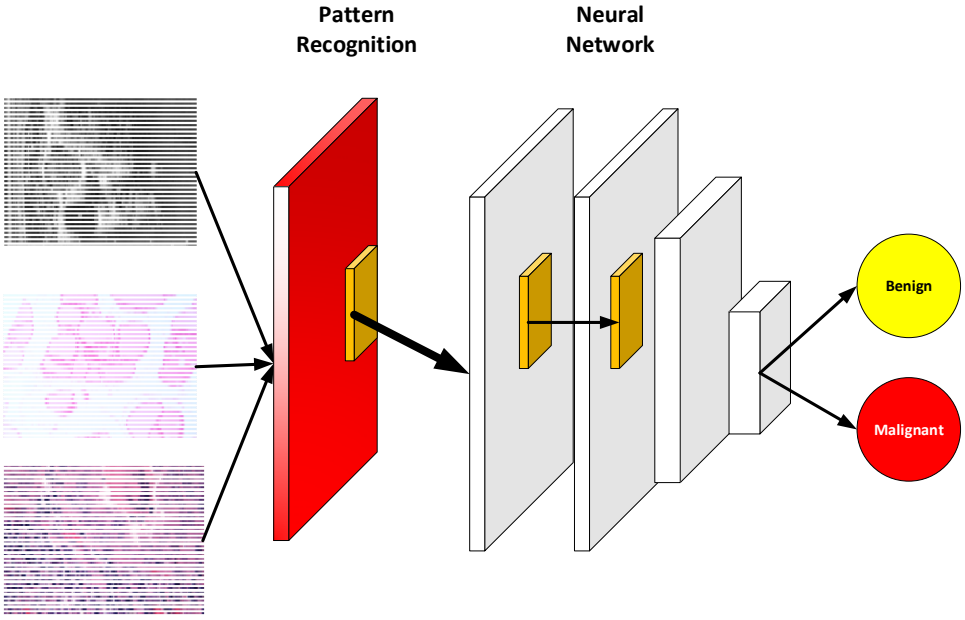

The above is a clear example of a pattern recognition system followed by a classifier. The classifier we have here is a neural network one but frankly we can use a variety of other classifier algorithms. It is critical to note that pure NN AI systems would just admit the images qua pixels. Here we add a priori knowledge of structures.

4 GENOMICS INTEGRATED

Everything we do with images whether those generated from processing to those observed directly are reflective of genomic consequences.

4.1 DNA

DNA sequencing has become a common practice. The literature is extensive and the sequencing may be complete or on segments of the total DNA.

4.1.1 Mixed Cells

Generally we see the sequencing done of a mass of cells. The problem is that type of sequencing reflects the mass and not the cell per se. One suspects as we can produce more cost effective single cell sequencing that the mixed cell approach will abate.

4.1.2 Single Cells

Single cell sequencing is now a possibility. Thus we can extract a cell at a time and sequence the individual cells. Then we get a complex array of sequenced data since in a tumor the DNA may be pleiomorphic[12]. As Navin et al noted:

Genomic analysis provides insights into the role of copy number variation in disease, but most methods are not designed to resolve mixed populations of cells. In tumours, where genetic heterogeneity is common1,2,3, very important information may be lost that would be useful for reconstructing evolutionary history. Here we show that with flow-sorted nuclei, whole genome amplification and next generation sequencing we can accurately quantify genomic copy number within an individual nucleus. We apply single-nucleus sequencing to investigate tumour population structure and evolution in two human breast cancer cases. Analysis of 100 single cells from a polygenomic tumour revealed three distinct clonal subpopulations that probably represent sequential clonal expansions.

Additional analysis of 100 single cells from a monogenomic primary tumour and its liver metastasis indicated that a single clonal expansion formed the primary tumour and seeded the metastasis. In both primary tumours, we also identified an unexpectedly abundant subpopulation of genetically diverse 'pseudodiploid' cells that do not travel to the metastatic site. In contrast to gradual models of tumour progression, our data indicate that tumours grow by punctuated clonal expansions with few persistent intermediates.

[12] See https://www.nature.com/articles/nature09807 Navin et al, Tumor Evolution Inferred by Single-cell Sequencing, Nature, 472, 90-94, 2001.

Single cell sequencing will introduce a massive data analysis challenge. If for example, we sequence 1,000 cells then we then must decide which ones are more important. Is there truly a stem cell and have we captured it and have we identified it?

4.2 RNA

RNA and its ensuing proteins are key elements we often examine. RNA however is often fragile and especially as it leaves the cell. Thus we often use a reverse transcriptase to obtain a CDNA from the RNA and use that as the means to identify the original RNA.

4.3 MIRNA

Micro RNAS have been found to be powerful elements controlling cells both locally and at a distance[13]. Micro RNAs have been known for about thirty years. During the last ten years there has been an explosion in the discovery, identification, and operation of these short stretches of single stranded RNAs. These small segments of RNA can act in powerful ways to silence gene expression by binding to mRNAs before they can effect actionable proteins or cutting them apart. This note is an attempt to examine the current status of these significant factor in cellular functioning and especially in cancer initiation, control and metastasis.

In early 2019 the paper by Alles et al noted:

While the number of human miRNA candidates continuously increases, only a few of them are completely characterized and experimentally validated. Toward determining the total number of true miRNAs, we employed a combined in silico high- and experimental low-throughput validation strategy.

We collected 28 866 human small RNA sequencing data sets containing 363.7 billion sequencing reads and excluded falsely annotated and low-quality data. Our high-throughput analysis identified 65% of 24 127 mature miRNA candidates as likely false-positives. Using northern blotting, we experimentally validated miRBase entries and novel miRNA candidates.

By exogenous overexpression of 108 precursors that encode 205 mature miRNAs, we confirmed 68.5% of the miRBase entries with the confirmation rate going up to 94.4% for the high-confidence entries and 18.3% of the novel miRNA candidates. Analyzing endogenous miRNAs, we verified the expression of 8 miRNAs in 12 different human cell lines.

In total, we extrapolated 2300 true human mature miRNAs, 1115 of which are currently annotated in miRBase V22. *The experimentally validated miRNAs will contribute to revising targetomes hypothesized by utilizing falsely annotated miRNAs.*

There are still many unanswered questions regarding miRNAs. For example:

[13] https://www.researchgate.net/publication/338684968_miRNAS_REDUX

1. What initiates the generation of an miRNA. The 2300 or so miRNAs are present in some cells and not others, and why.

2. What are the promoters and initiators of these miRNA transcriptions. Are there upstream genetic characteristics and elements that make for their transcription.

3. miRNAs can inhibit transcribed mRNA thus inhibiting translation. What is the overall chemical reactivity of each which dominates. For example, if a cell can produce 1 miRNA per day but it can produce 2 mRNA per day, perhaps only half are blocked and there would be a de minimis effect. On the otherhand if the miRNA can survive the mRNA degradation then it has a perpetual existence. The reaction dynamics of this overall process is yet to be understood.

4. In cancers, we have identified a set of miRNAs, many of which are common across a large set of malignancies. The question is; is the driver of the malignant process the miRNA or some upstream genetic action?

5. Why do some cells activate miRNAs and others do not?

6. Can we develop upstream and downstream maps for any miRNA?

7. Is there a stochiometric system for the analysis of miRNA interactions?

8. As miRNAs flow from the nucleus (as works in progress), what are the detailed steps by which they may be mitigated against.

9. The relationships between the up and down stream elements and the related miRNAs have a dynamic characteristic where concentrations of each entity in such a chain could be characterized. Can this be ascertained and demonstrated?

10. Are miRNA, as well as up and down stream entities targetable by therapeutics and if so how.

11. Targeting as above, what are the "unintended consequences" across homeostatic processes?

12. miRNAs via exosomes or even directly can be effectors of metastasis. How is this accomplished and how can it be mitigated?

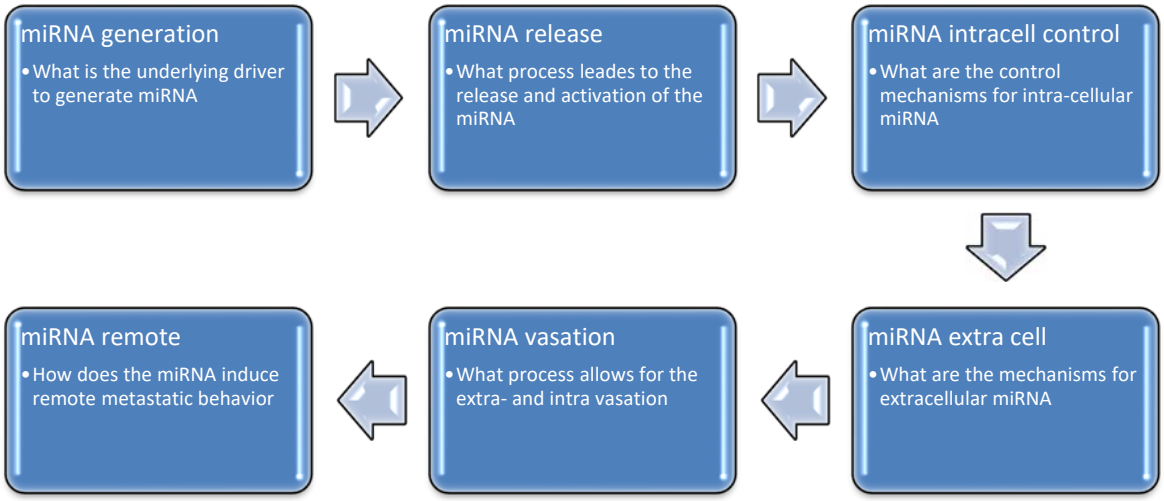

In this note our objective is to overview the miRNA status, examine the miRNAs for a set of malignancies, overview the methodology to measure these miRNAs and then to explore the options to link the measurements to diagnostic and prognostic measures.

The challenges we see facing this effort clinically are:

1. Identification of miRNAs and malignant states

2. Measurement of the miRNAs in an effective and reasonable cot manner

3. The ability to identify a specific lesion despite the prolific presence of miRNAs across many possible ones.

4. The development of a metric which maps the miRNA measures into diagnostic and prognostic results by lesion type.

5 CANCERS

We now examine the interaction of radiomic studies in the context of various malignancies. Our interest is not any specific image modality but an analysis by cancer of the options available and the processes which can be employed to obtain diagnostic data from the images.

Now with these images, radiological, cytological, histological, and others we can find metrics which have been developed to stage and diagnose various organ growths. Classically these metrics relied upon features which the observer can identify and then use as a probable marker for a malignancy. For the most part no single market has optimum specificity and sensitivity.

5.1 PROSTATE

Prostate cancer is one of the highest occurring malignancies in men[14]. It generally is slow growing but also has the ability to hide itself due to less than adequate means of being identified. The PSA test has been used for nearly thirty years and it is somewhat satisfactory. It has been abashed by various Government groups because it is not perfect enough but it had saved lives. Its use has declined and in turn mortality has increased. We have argued that the research upon which the withdrawal of PSA is fatally flawed. We leave that for other arguments.

5.1.1 The PSA Test

We consider a simple test under current use. Namely the 4K Test[15]. The 4K test is described somewhat in the papers by Bryant et al (2015) and Stattin et al (2015) and also in the 4K web site as indicated. Basically, the following data is measured and entered:

1. Total PSA, tPSA
2. Free PSA, fPSA
3. Intact PSA, iPSA[16]
4. hk2 (or KLK2), hk2
5. Age, A
6. DRE, DRE
7. Prior Biopsy Status, PBS

Then a score is determined by a functional means as follows:

[14] https://www.researchgate.net/publication/264960277_Prostate_Cancer_A_Systems_Approach This is a 2013 document. On the Research Gate website there are many more which bring much of this up to date.

[15] https://www.4kscore.com/

[16] Note from the OPKO Brochure they state: *The iPSA test is a sandwich (noncompetitive) immunoassay that employs two distinct mouse monoclonal antibody products. The capture probe is a biotinylated, recombinant His6-Cys-tagged Fab fragment of the monoclonal antibody 5A10 with specificity for fPSA (of which iPSA is a component). The tracer is a Europium-labelled monoclonal antibody 4D4, with specificity to iPSA and complexed PSA (PSA-ACT). In combination, the reagents are specific for iPSA.*

$$f_{4K}(x) = f(tPSA, fPSA, iPSA, hk2, A, DER, PBS)$$

Just what that equation specifics are is considered proprietary. However the result is a number or percent that relates to a contemporaneous biopsy report. Namely f_{4K} equals:

$$f_{4K} = P\left[\text{Biopsy is Gleason 7 or higher and distant metastasis}\right] + n$$
$$n = error$$

Namely the f number in a 4K measurement reflects the probability of there being an existing malignancy of considerable status and that the malignancy will lead to death in 20 years. The score goes from <1% to 95%.

Now the ROC AUC for this test is 0.82.

Let us examine this a bit from a statistical perspective.

First let us look at the PSA alone. It may look as follows.

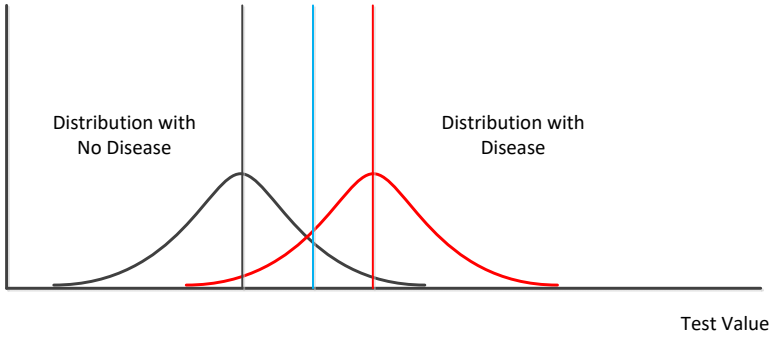

P[D]=P[Say Disease | Disease Present]
P[FA]=P[Say Disease | No Disease Present]

Here we have a PSA threshold of say 4.0. Now with this test we have many diseased states below 4.0 and many non-diseased states above. The red curve is the distribution of PSA give a PCa and the black is the PSA with no PCa. We could vary the blue decision line to try to change things but when we do we see poor performance. We could plot the Sensitivity vs the 1-Specificity of a PSA test as shown below:

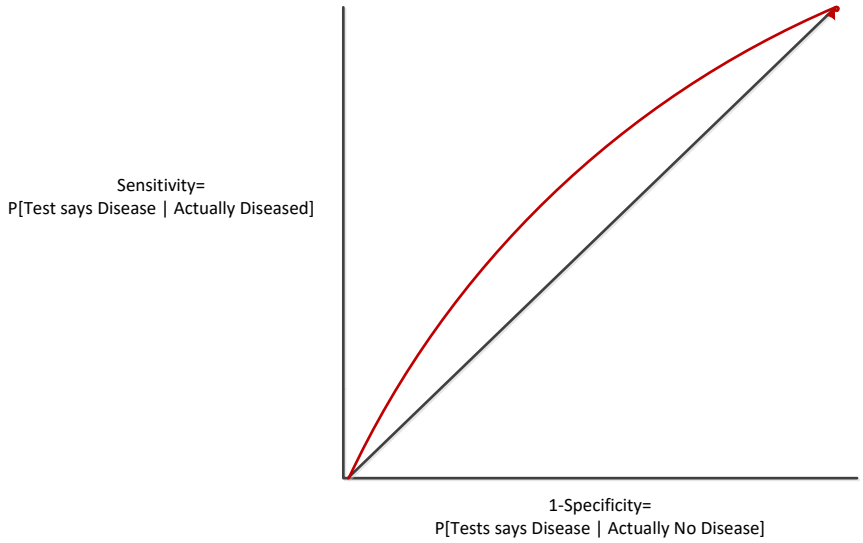

What this states is that as we try to get better detection we get poorer False Alarm rates. The red curve is almost linear and that means that if we want a 90% detection probability then we will suffer almost a 90% False Alarm rate. The measure of performance is the Area Under the Curve, AUC. The worst case AUC is a straight line, a coin toss if you will, and is 0.5.

Now with 4K one alleges gets a better discriminant. We depict that situation below:

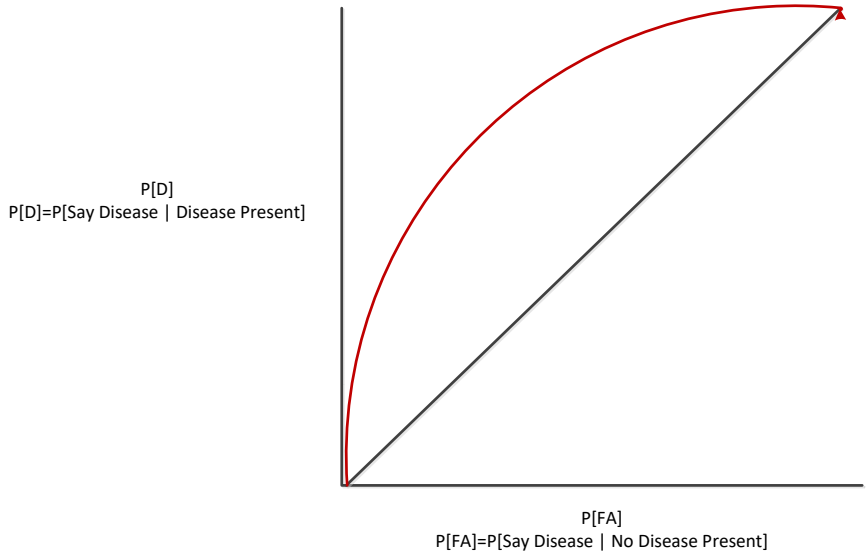

Note that we now can get excellent Detection rates while suffering low False Alarm Rates. This means that the 4K tests look like the one below:

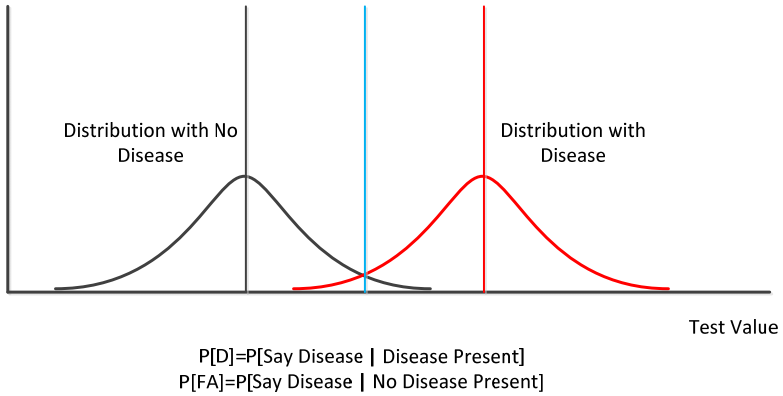

That is the distributions for disease and no disease are further apart and/or their variance or noise levels are lower.

This means that we have a much greater AUC and 4K argues for an 0.82 or higher AUC.

Now we may have some issues with 4K. On the positive side it has gone through many tests. On the negative side:

1. It does not include temporal data. No velocity measurements are included. One may then ask if velocity is a key measure. As we have shown before, for example, HbA1c may affect PSA and perhaps that should be normalized.

2. It avoids prostate volume. As we have also shown before volume is a key metric, just by definition.

3. It ignores family history. That is strange since as is well known family history is a significant factor.

4. Also recall that if the test says 1% probability of disease then we have:

$$PD = P[\text{Say Disease}|\text{Disease}]$$

$$PFA = P[\text{Say Disease}|\text{No Disease}]$$

but

$$P[\text{Say Disease}|\text{Disease}][[\ ]]P[\text{Disease}] = P[\text{Disease}|\text{Say Disease}]P[\text{Say Disease}]$$

or

$$P[\text{Say Disease}|\text{Disease}] = \frac{P[\text{Disease}|\text{Say Disease}]P[\text{Say Disease}]}{P[\text{Disease}]}$$

or

$$P[\text{Disease}|\text{Say Disease}] = \frac{P[\text{Say Disease}|\text{Disease}]P[\text{Disease}]}{P[\text{Say Disease}]}$$

but

$$P[\text{Say Disease}] = P[\text{Say Disease}|\text{Disease}]P[\text{Disease}] + P[\text{Say Disease}|\text{No Disease}]P[\text{No Disease}]$$

or

$$P[\text{Say Disease}] = PDp + PFA(1-p)$$

where

$$p = P[\text{Disease}]$$

Thus is PD is high and PFA is low, which occurs with a large AUC, then PD is almost p. Likewise, PND, probability of no disease given disease, is likewise low if we say it is low.

Yet the overall performance of the test is quite impressive.

Heger Table:

Parameter	**Mean Cancer**	**SD Cancer**	**Mean Normal**	**SD Normal**
K^+	**5.73**	**3.84**	**8.03**	**4.08**
Na^+	13.18	8.12	10.62	4.38
Cl^-	9.12	6.98	9.98	4.14
Uric acid	**15.44**	**57.95**	**0.26**	**0.10**
Urea	**38.66**	**18.42**	**23.79**	**12.26**
PSA	**4.93**	**7.52**	**0.00**	**0.00**
Glucose	0.05	0.13	0.02	0.02
Pyrogallol	0.08	0.21	0.00	0.00
fPSA	**17.46**	**2.12**	**0.00**	**0.00**
pH	6.05	0.75	6.49	0.32
Creatinine	**15.04**	**4.74**	**9.57**	**18.94**

5.1.2 mpMRI

mpMRI has gained considerable acceptance in the diagnosis of PCa. As Stabile et al report:

1. *Multiparametric MRI (mpMRI) of the prostate is a novel promising tool for diagnosis of prostate cancer that might help to reduce overdiagnosis of insignificant prostate cancer.*

2. *mpMRI should include four sequences: T1-weighted images, T2-weighted images, diffusion-weighted images (DWI) and dynamic contrast-enhanced imaging (DCEI).*

3. *Interpretation and reporting of mpMRI must be carried out following standardized scoring systems (such as Prostate Imaging Reporting and Data System (PI-RADS) v2).*

4. *The use of mpMRI is considered useful; the use of mpMRI-targeted biopsy is increasing the detection of clinically significant prostate cancer in both biopsy-naive and previous negative biopsy settings.*

5. *The use of mpMRI as a triage test is still controversial. In men with negative mpMRI, omitting a biopsy can only be considered when the clinical suspicion of prostate cancer is low.*

6. *Improvements in inter-reader agreement, development of computer-aided diagnostic systems and assessment of biomarkers to use in combination with mpMRI are needed.*

Currently mpMRI scoring for PCa is done with PI-RADS[17]. PIRADS is a complex integrated system which rates the entire prostate in peripheral and transition zone. It may appear as follows:

[17] https://www.acr.org/Clinical-Resources/Reporting-and-Data-Systems/PI-RADS

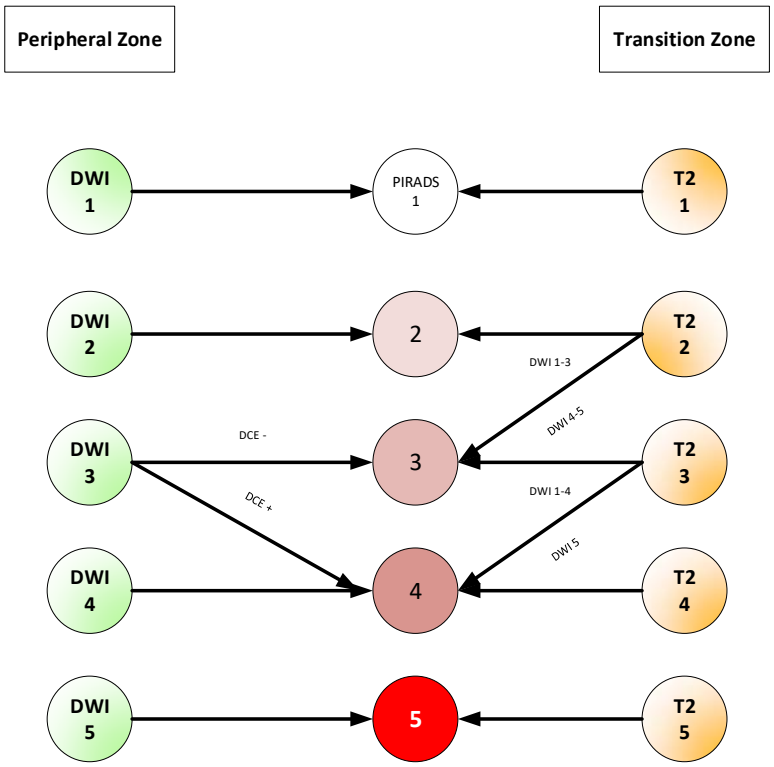

where the entries are defined as[18]: Now it must be understood that the above PI-RADS does have significant margins of errors especially if there have been multiple previous biopsies. This seems to be due to the resulting scar tissues created which in many ways appear as a putative malignancy.

The basis for interpreting mpMRI on diagnosing PCa is as follows:

1. T2 WEIGHTED IMAGING (T2W) SCORE

I. TRANSITION ZONE

1: normal appearing transition zone (rare) or a round, completely encapsulated nodule ("typical nodule" of benign prostatic hyperplasia)

2: a mostly encapsulated nodule or a homogeneous circumscribed nodule without encapsulation ("atypical nodule"), or a homogeneous mildly hypointense area between nodules

3: heterogeneous signal intensity with obscured margins; includes others that do not qualify as 2, 4, or 5

[18] https://radiopaedia.org/articles/prostate-imaging-reporting-and-data-system-pi-rads-1?lang=us

4: lenticular or non-circumscribed, homogenous, moderately hypointense, and <1.5 cm in greatest dimension
5: same as 4, but ≥1.5 cm in greatest dimension or definite extra prostatic extension/invasive behavior

For transition zone lesions, the overall PI-RADS assessment usually follows the T2W score, but scores of 2 or 3 can be upgraded by the DWI (see below).

II. PERIPHERAL ZONE

1: uniform high signal intensity (normal)
2: linear or wedge-shaped hypointensity or diffuse mild hypointensity, usually indistinct margin
3: heterogeneous signal intensity or non-circumscribed, rounded, moderate hypointensity; includes others that do not qualify as 2, 4, or 5
4: circumscribed, homogenous, moderate hypointensity, and <1.5 cm in greatest dimension
5: same as 4 but ≥1.5 cm in greatest dimension or definite extra prostatic extension/invasive behavior

For peripheral zone lesions, the T2W score is only used for the overall PI-RADS assessment if the DWI is inadequate or absent. Scores of 3 can be upgraded by presence of dynamic contrast enhancement.

2. DIFFUSION WEIGHTED IMAGING (DWI) SCORE

Signal intensity in the lesion is visually compared to the average signal of normal prostate tissue elsewhere in the same histologic zone.

I. TRANSITION ZONE OR PERIPHERAL ZONE

1: no abnormality on ADC or high b-value DWI
2: linear/wedge shaped, hypointensity on ADC and/or hyperintensity on high b-value DWI
3: focal (discrete and different from background), mild/moderate hypointensity on ADC and/or mild/moderate hyperintensity on high b-value DWI; may be markedly hypointense on ADC or markedly hyperintense on high b-value DWI, but not both
4: focal, marked hypointensity on ADC and marked hyperintensity on high b-value DWI; <1.5 cm in greatest dimension
5: same as 4 but ≥1.5 cm in greatest dimension or definite extra prostatic extension/invasive behavior

For peripheral zone lesions, the overall PI-RADS assessment usually follows the DWI score, but a score of 3 can be upgraded by the presence of dynamic contrast enhancement (see below).

For transition zone lesions with a T2W score of 2 or 3, a DWI score that is two higher (i.e. 4 or 5, respectively) is used to upgrade the overall PI-RADS assessment by one point (i.e. to 3 or 4, respectively).

3. DYNAMIC CONTRAST ENHANCEMENT (DCE)

I. (-) NEGATIVE:

no early or contemporaneous enhancement, or
diffuse multifocal enhancement not corresponding to a focal finding on T2W and/or DWI, or
focal enhancement corresponding to a lesion demonstrating features of benign prostatic hyperplasia on T2W (including features of extruded benign prostatic hyperplasia nodule in the peripheral zone)

II. (+) POSITIVE:

focal, and
earlier than or contemporaneous with enhancement of adjacent normal prostatic tissues, and
corresponds to suspicious finding on T2 and/or DWI

For peripheral zone lesions with DWI score of 3, the presence of dynamic contrast enhancement is used to upgrade the overall PI-RADS assessment category to 4.

The resulting categories are:

PI-RADS™ v2.1 Assessment Categories

PIRADS 1 – Very low (clinically significant cancer is highly unlikely to be present)
PIRADS 2 – Low (clinically significant cancer is unlikely to be present)
PIRADS 3 – Intermediate (the presence of clinically significant cancer is equivocal)
PIRADS 4 – High (clinically significant cancer is likely to be present)
PIRADS 5 – Very high (clinically significant cancer is highly likely to be present)

From the work of Ghai and Haider we have the following mpMRI example. The note:

A 55-year-old man with Gleason 7 (4 + 3) prostate cancer. (a) Axial T2-weighted image (T2WI) shows the normal hyperintense T2 signal in the peripheral zone (white arrow) from the high water content with cancer (black arrow) appearing as an area of low signal on T2WI. (b) Apparent diffusion coefficient map at the same level showing low signal from the restricted diffusion at the site of cancer (arrow)...

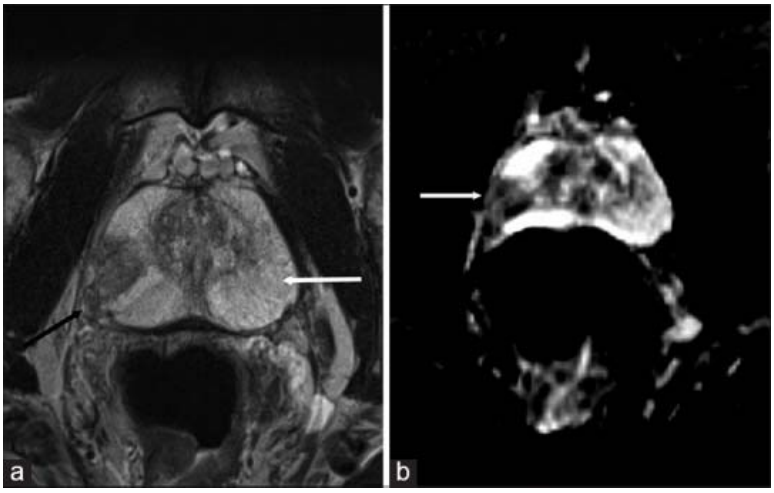

As Monti et al have recently noted:

Recently, the use of a multiparametric Magnetic Resonance Imaging (mpMRI) approach, combining anatomic T1 or T2-weighted (T2W) images with functional MRI methods as Diffusion Weighted Imaging (DWI) and Dynamic Contrast Enhanced (DCE) imaging, provided substantial improvements in non-invasive prostate cancer detection and characterization.

In fact, the imaging approach, besides its non-invasiveness, can give "in vivo" information on the entire tumor volume, thereby reducing inaccuracies due to sampling errors in histopathological analyses. The Prostate Imaging-Reporting and Data System (PI-RADS) was developed in 2013, and then updated in 2015 (PI-RADS v2) [5], in order to standardize the use of mpMRI in PCa imaging. This technology provides a scale indicating how likely an mpMRI finding from T2W, DWI, and DCE is related to a clinically significant cancer.

The PI-RADS score ranges from one, which indicates a very low probability of malignancy, to five, which indicates a very high probability that a lesion is malignant. Since its introduction, the PI-RADS classification has played a very important role in PCa diagnosis, proving to be a useful tool for the detection of prostatic lesions and their characterization in terms of aggressiveness. However, due to its definition, PI-RADS scoring can be affected by subjectivity and inter-/intra-operator variability, which are factors that may compromise PCa assessment. Moreover, it is not unusual to find benign and malignant lesions with similar imaging findings, making it challenging to detect the nature of prostatic lesions.

It should also be considered that lesions classified as having a PI-RADS score of three are usually lesions termed as "intermediate" or "equivocal on the presence of clinically significant cancer". The abovementioned limitations of PI-RADS, together with an ever-growing volume of medical images for each patient and the development of increasingly powerful image acquisition and processing techniques, have led to an increasing interest in new quantitative approaches to analyze mpMRI images
Fehr et al have noted:

Our work demonstrates that PCa diagnosis can be improved by combining data-augmented classification together with more of the latent information in standard MRIs (the so-called "radiomics hypothesis") (27, 28) compared with using ADC mean or T2 signal intensities alone, thereby reducing the potential for under- or overdiagnosis. Fig. 1 A and B show the ADC energy, ADC entropy, T2 energy, and T2 entropy overlaid on a slice of the ADC and corresponding T2-w MR image for two different patients: one with a tumor of GS 6ð3 + 3Þ and the other with a tumor of GS 9ð4 + 5Þ. …the energy and entropy values computed from different tumor types appear to be very different, which suggests that textures, in combination with ADC, can help to differentiate between the cancer type…

Our results suggest that with sample augmentation, reasonably accurate classification with high sensitivity and specificity can be obtained, even for highly imbalanced data such as in the classification of cancer GS. Our work also showed that texture features computed from both ADC and T2-w images drastically improve the classification performance than just the ADC mean and T2 mean.

Finally, incorporating the interaction of image features for feature selection followed by a classification method (RFE-SVM) achieved the highest classification accuracy.

Wang et al have noted:

Multiparametric (MP) magnetic resonance imaging (MRI) may improve the diagnosis and the care of PCa patients by providing morphological and functional information about the prostate. MRI sequences shown to correlate with properties associated with PCa include T2-weighted imaging (T2WI), diffusion-weighted imaging (DWI), MR spectroscopy, and dynamic contrast-enhanced (DCE) MRI. MP-MRI is especially effective in revealing anterior prostate cancer in men with negative random transrectal 12- core biopsy . In such cases, MP-MRI is beneficial for selecting men who should undergo anterior biopsy. Such an approach increases the positive predictive power of PCa diagnosis .

It is therefore highly recommended that MP-MRI is used rather than a single MRI modality when assessing a patient for prostate lesions. By fusing endorectal coil MR images to a preprocedure TRUS using electromagnetic needle tracking, biopsies may be directed to suspicious lesions and the location of biopsies may be documented . Targeted prostate biopsy with MPMRI guidance has been shown to improve the sensitivity of prostate cancer detection when compared with random biopsy. MP-MRI/ultrasound image fusion reduces the number of required biopsies while also reducing the diagnosis of clinically insignificant cancer . Initially, endorectal coils were used during MP-MRI to increase the signal-to-noise ratio (SNR). However, as MP-MRI has become more widespread and technology has improved, endorectal coils are no longer consistently used and the costs associated with them are avoided .

Futterer et al. found AUC to be significantly higher when endorectal coils were used when compared with pelvic coils. Similarly, Turkbey et al. found that more cancer foci were detected using dualcoil prostate MRI than when nonendorectal coil MRI was used at 3T . However, Bratan et al. contends this claim with findings that the field strength and the type of imaging coils used have no significant influence on the detection rate of tumors.

As technology evolves it is likely that there will be a decreasing need for endorectal coils. 3. Computer Aided-Diagnosis for Prostate Cancer Interpreting MRI requires a high level of expertise and is time consuming. Significant interobserver variation and a lack of sensitivity, specificity, and accuracy exist for radiologists in interpreting the volume and stage of lesions in prostate MRI [36–38]. Multiparametric MRI T2WI ADC · · ·

Ktrans Registration Prostate CADx workflow Diagnosis results Classification Feature extraction Candidate generation Segmentation (prostate, central gland) Preprocessing (T2WI, ADC, Ktrans, etc.) Figure 1: Workflow of a typical prostate CADx system. Green rectangles indicate data (original scans and images after preprocessing); yellow rectangles indicate processes applied to the data or images. There is demand for an accurate computer aideddiagnosis (CADx) system that decreases reading time, reduces required expertise in radiology reading, and offers a consistent risk assessment of cancer presence in prostate MRI. Such a CADx system could automatically detect suspicious lesions in prostate MR images to help screen for prostate cancer in large patient populations. A typical CADx system for prostate cancer detection takes multiparametric MR images (MP-MRI), processes them, and generates a specific diagnostic result (e.g., a prediction map of the prostate showing regions with high probability to be cancer).

There are some common components which are shared by prostate CADx systems such as feature extraction and classification

Wang et al demonstrate a workflow for a prototypical PCa automated system as below:

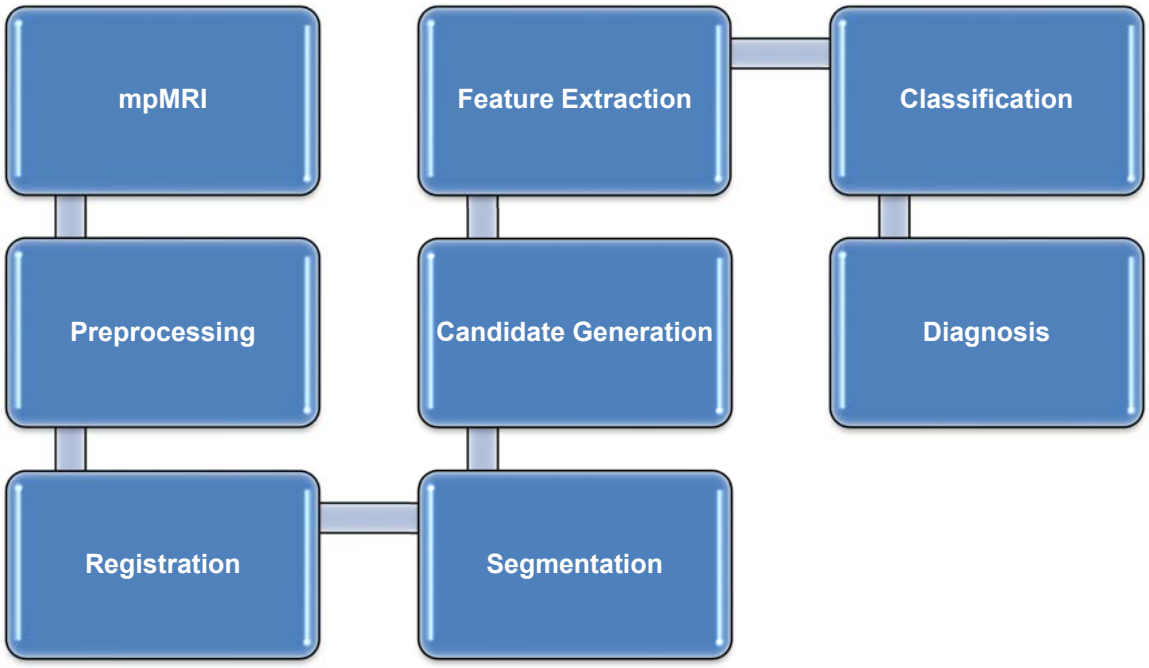

A recent result by Ahdoot et al has demonstrated the efficacy of the integrate approach. The authors note:

Among patients with MRI-visible prostate lesions, the addition of MRI-targeted biopsy to systematic biopsy increased the detection of clinically significant cancers (grade group ≥3) and led to a net decrease in the detection of clinically insignificant cancers. Although many of these benefits resulted from MRI-targeted biopsy alone, omission of systematic biopsy would have led to missing the diagnosis of 8.8% of clinically significant cancers. Furthermore, among the patients who underwent subsequent radical prostatectomy, combined biopsy was associated with the lowest rate of upgrading of the cancer grade group between biopsy and wholemount histopathological analysis. Collectively, these findings suggest that combined biopsy provides improved diagnostic accuracy over either systematic or MRI-targeted biopsy alone and better predicts the results of final histopathological analysis.

However, the major lacking result was the percent who had PI-RADS of 3-5 who when biopsied showed no signs of malignancy. We feel that such a metric is essential and from clinical results it occurs especially in patients with multiple prior biopsies.

5.1.3 US

Ultrasound is used principally in prostate biopsy. Currently this is integrated with mpMRI images and its significantly improves the overall performance.

5.1.4 Biopsy

Prostate biopsies occur in two stages. First is the needle biopsy taken to assess the patient's condition and perform an initial staging. Second, upon removal of the prostate, if such is possible, then a final overall biopsy is performed.

A benign view is shown below. Note the basal and luminal cells[19].

[19] See Epstein Figure 3.4 for a benign prostate cell

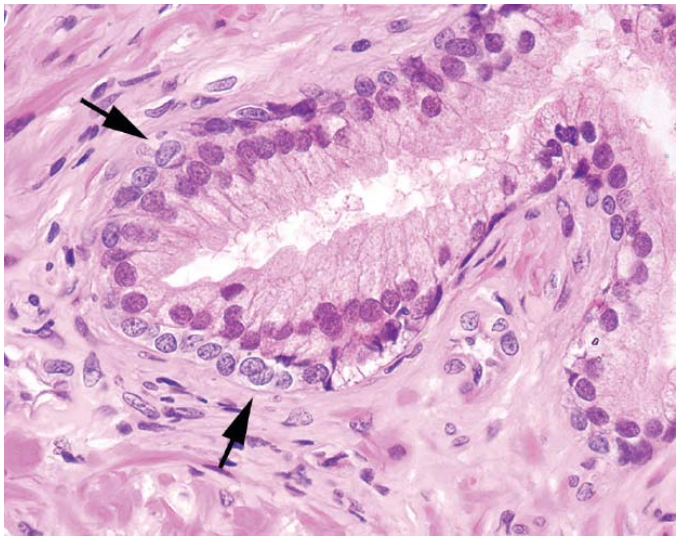

The adenocarcinomas for various grades, Gleason, are shown below (from Epstein):

Note that the increase in Gleason grading is reflected in a loss of structure and a movement to a diffuse sheet of tumor cells.

5.1.5 Genomics

Stoyanova et al have noted:

Standard clinicopathological variables are inadequate for optimal management of prostate cancer patients. While genomic classifiers have improved patient risk classification, the multifocality and heterogeneity of prostate cancer can confound pre-treatment assessment. The objective was to investigate the association of multiparametric (mp)MRI quantitative features with prostate cancer risk gene expression profiles in mpMRI-guided biopsies tissues. Global gene expression profiles were generated from 17 mpMRI-directed diagnostic prostate biopsies using an Affimetrix platform. Spatially distinct imaging areas ('habitats') were identified on MRI/3D-Ultrasound fusion. Radiomic features were extracted from biopsy regions and normal appearing tissues. We correlated 49 radiomic features with three clinically available gene signatures associated with adverse outcome.

The signatures contain genes that are over-expressed in aggressive prostate cancers and genes that are under-expressed in aggressive prostate cancers. There were significant correlations between these genes and quantitative imaging features, indicating the presence of prostate cancer prognostic signal in the radiomic features. Strong associations were also found between the radiomic features and significantly expressed genes. Gene ontology analysis identified specific radiomic features associated with immune/inflammatory response, metabolism, cell and biological adhesion. To our knowledge, this is the first study to correlate radiogenomic parameters with prostate cancer in men with MRI-guided biopsy

The overall procedure in PCa diagnosis can thus be indicated as follows:

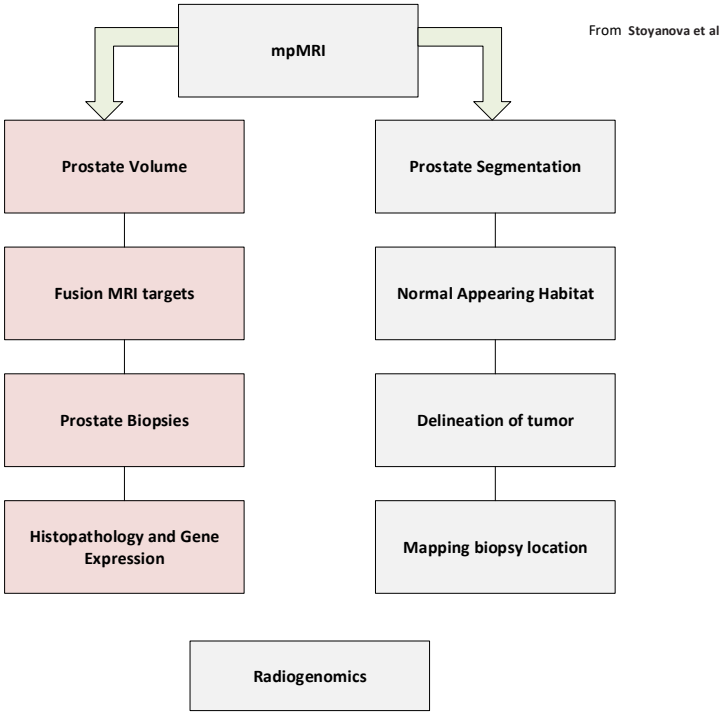

From the perspective of involved genes in PCA we have the list:

1. p53
2. RB1
3. AR
4. PTEN
5. MYC
6. TMPRSS2:ETS
7. TMPRSS2:ERG
8. SPOP

to name a few. There is also methylation issues and miRNAs as well.

5.2 BREAST

Breast cancer is the most significant cancer in women in the U.S. It is however like many cancers multifaceted. Ductal carcinoma in situ is often treated as aggressively as more advance forms. For decades now women have been asked to undergo breast exams in hopes of identifying the disease early. This seems to have worked but it also has identified DIC.

As Kuhl had noted recently (2015):

Breast imaging is special. Nowhere else, possibly with the sole exception of dedicated interventional radiology, is the radiologist as visible as in the breast imaging arena. Here, the radiologist is integrated in a multidisciplinary team, where he or she is recognized as a physician who assumes direct and personal patient responsibility and genuinely cares for patients. The radiologist may accompany a woman for many years for screening. When signs or symptoms of breast cancer arise, or in case a screening abnormality is found, the radiologist will be the first to discuss these findings with the patient and her family. It is usually the radiologist alone who decides whether biopsy is needed or not.

He or she will then do the biopsy and discuss the pathology results with the patient, her family, and other health care providers. The radiologist is experienced in communicating to a patient and her family that breast cancer is present, and knows how to respond to sorrow and anxieties. The radiologist will then, often enough, be asked to help find a breast surgeon for the patient and will thus become a referring physician for other disciplines.

5.2.1 Classic Methods

The classic method of identifying breast cancer is via plain film x rays albeit using flat screen capture methods. As Kuhl et al (2005) had noted:

Mammography alone, and also mammography combined with breast ultrasound, seems insufficient for early diagnosis of breast cancer in women who are at increased familial risk with or without documented BRCA mutation. If MRI is used for surveillance, diagnosis of intraductal

and invasive familial or hereditary cancer is achieved with a significantly higher sensitivity and at a more favorable stage.

Thus the use of MRI, especially mpMRI is highly suggestive.

5.2.2 mpMRI

mpMRI, as we have discussed is a complex imaging technique that combines the three elements of T2 scans, diffusion determination, and dynamic contrast tracking in an attempt to identify lesions.

From Fan et al:

The purpose of this study was to investigate the role of features derived from breast dynamic contrast-enhanced magnetic resonance imaging (DCE-MRI) and to incorporated clinical information to predict the molecular subtypes of breast cancer. In particular, 60 breast cancers with the following four molecular subtypes were analyzed: luminal A, luminal B, human epidermal growth factor receptor-2 (HER2)-over-expressing and basal-like. The breast region was segmented and the suspicious tumor was depicted on sequentially scanned MR images from each case. In total, 90 features were obtained, including 88 imaging features related to morphology and texture as well as dynamic features from tumor and background parenchymal enhancement (BPE) and 2 clinical information-based parameters, namely, age and menopausal status. An evolutionary algorithm was used to select an optimal subset of features for classification.

Using these features, we trained a multi-class logistic regression classifier that calculated the area under the receiver operating characteristic curve (AUC). The results of a prediction model using 24 selected features showed high overall classification performance, with an AUC value of 0.869. The predictive model discriminated among the luminal A, luminal B, HER2 and basal-like subtypes, with AUC values of 0.867, 0.786, 0.888 and 0.923, respectively. An additional independent dataset with 36 patients was utilized to validate the results. A similar classification analysis of the validation dataset showed an AUC of 0.872 using 15 image features, 10 of which were identical to those from the first cohort. We identified clinical information and 3D imaging features from DCE-MRI as candidate biomarkers for discriminating among four molecular subtypes of breast cancer.

In addition Kuhl (2015) had noted:

Since tumor biology (molecular subtyping) has replaced previous criteria for prognostic evaluation as well as previous concepts for treatment allocation, there is a growing interest in establishing innovative breast imaging methods, in particular, contemporary magnetic resonance–based in vivo imaging biomarkers, to help classify tumor biology. Such techniques are diffusion-weighted imaging (DWI) and its derivatives like diffusion kurtosis imaging and intravoxel incoherent motion imaging, DCE-MRI and its kinetic analyses, and 1H or 31P MR spectroscopy, all of which can be combined into so-called multiparametric (mp) breast MRI protocols.

For instance, specifically high-grade tumors or tumors with high (Ki-67) proliferation fraction are usually hypercellular compared with surrounding normal breast tissue, which translates into restricted diffusion of free water molecules on DWI. Mori et al50 have indeed shown that ADC values correlate with proliferation rates in luminal-B cancers. The increased cellular (i.e., membrane) turnover in rapidly growing tumors will lead to a detectable choline peak in proton MR spectroscopy. Tumors need to maintain this growth by increasing their local supply with oxygen and nutrients.

This is achieved by releasing peptides like vascular endothelial growth factor that induce local angiogenesis. Angiogenesis leads to a fundamental change of a tumor's microvascular architecture, with sprouting of existing vessels as well as development of de novo formed vessels, usually with fenestrated vessel wall linings that go along with increased vessel permeability. The increased metabolic turnover leads to an increased amount of toxic waste products that are removed through dilated drainage veins.

The increased perfusion leads to the well-known strong and early enhancement in DCE-MRI, and the increased permeability, together with the efficient venous drainage, cause the washout time course that is characteristic of breast cancer.18,62 It has been shown that DCE-derived enhancement kinetics correlate with estrogen receptor status, HER2- status, nuclear grade/Ki-67, and epidermal growth factor receptor expression. The increased permeability leads to leakage of larger molecules such as proteins from the intravascular to the interstitial space, which will increase the oncotic (colloid-osmotic) pressure within the cancer, a fact that drags water from the intravascular into the interstitial space and thus increases the interstitial water volume fraction. This, in turn, will correlate with a cancer's signal in T2-weighted imaging. If angiogenesis fails or is insufficient to reach the innermost cell layers of a cancer, then hypoxia will occur, again detectable through the tumor's internal architecture of enhancement in DCE-MRI (rim enhancement), or through blood oxygenation level dependent contrast MRI.

Since the pulse sequences that provide such "functional" information are usually associated with borderline signal-to-noise ratio, use of higher magnetic fields such as 3.0 T or, more recently, even 7.0 T, promises an even more accurate and extensive assessment of tumor biology. Visualization of such functional information is useful in clinical practice for a number of purposes.

First, it can be exploited for further differential diagnosis of enhancing lesions seen in breast MRI, that is, for the further differentiation of benign, high-risk, and malignant lesions in breast MRI. The combination of high-resolution cross-sectional morphology, enhancement kinetics, a lesion's signal in T2-weighted images and in DWIs leads to a high specificity and positive predictive value of contemporary breast MRI protocols. Even regular 1.5-T breast DCE-MRI protocols are inherently "multiparametric" compared with, for example, mammography or DBT. The diagnostic accuracy achieved with such protocol is sufficient to be used for so-called problem solving. Accordingly, and in contrast to currently held beliefs, we have recently shown that breast MRI can indeed be used to definitely settle screen-detected mammographic or ultrasound findings and thus help avoid unnecessary biopsy.

Second, such functional imaging methods promise to provide additional independent diagnostic information that adds to our understanding of a cancer's ability to grow and metastasize. The current focus on tumor genomics ignores the fact that successful tumor growth does not only depend on a tumor's genomic toolbox but also on its microenvironment, that is, features of the tissue that hosts the cancer. The interaction between a cancer and its microenvironment, and the degree to which a cancer is successfully shaping its environment to sustain its growth, are probably best assessed by noninvasive in vivo functional imaging. Accordingly, we propose that in the future, such mp MRI techniques will be used to help amend the assessment of a tumor's aggressiveness and its biologic and prognostic importance.

Third, an established clinical situation where mp breast MRI is used is to monitor response to systemic treatment.

5.2.3 Biopsy and Images

We show some of the biopsy images and radiation images as follows. Below we show a histological slide of breast cancer[20].

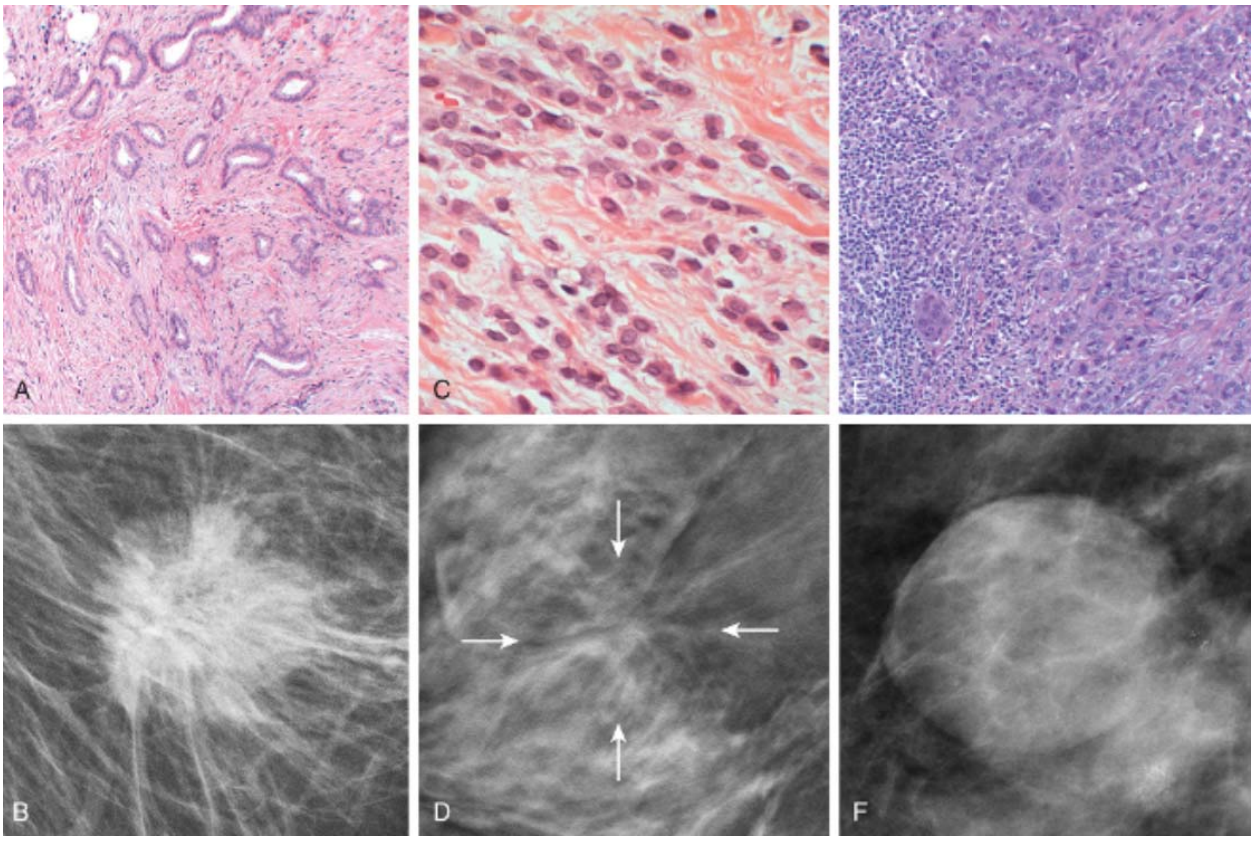

[20] See Kumar et al, Fig 19.29

Now we can also consider a single lesion as shown below and examine how we can process it for a discriminant. First the lesion:

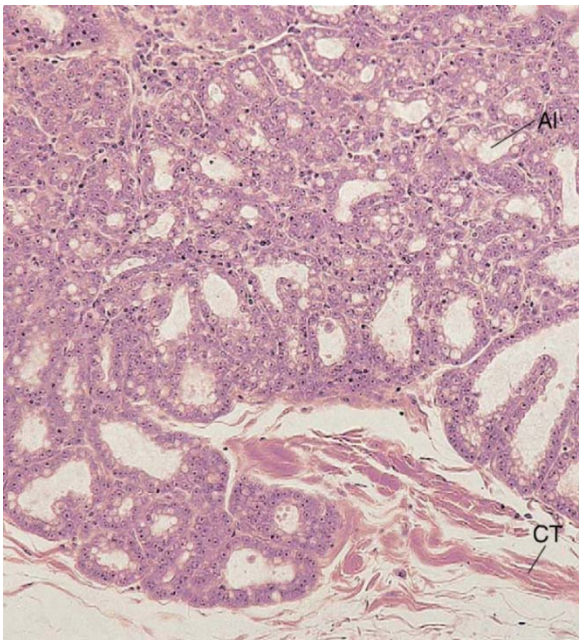

Using image enhancements we show below the edge profiling of the previous slide. This processed image may thus be one of several images processed to be used in an identifier.

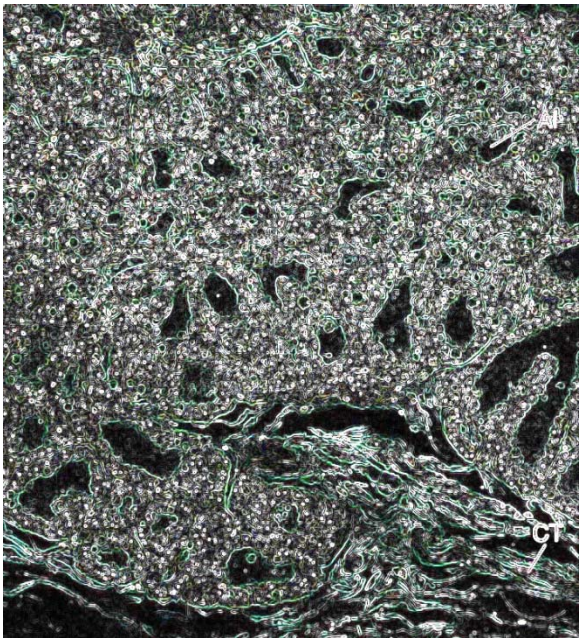

This processing is an example of image reduction. Here the reduction is quite complex.
An x ray image is shown below. This is typical showing a lesion. This is a prominent lesion and most likely somewhat advanced.

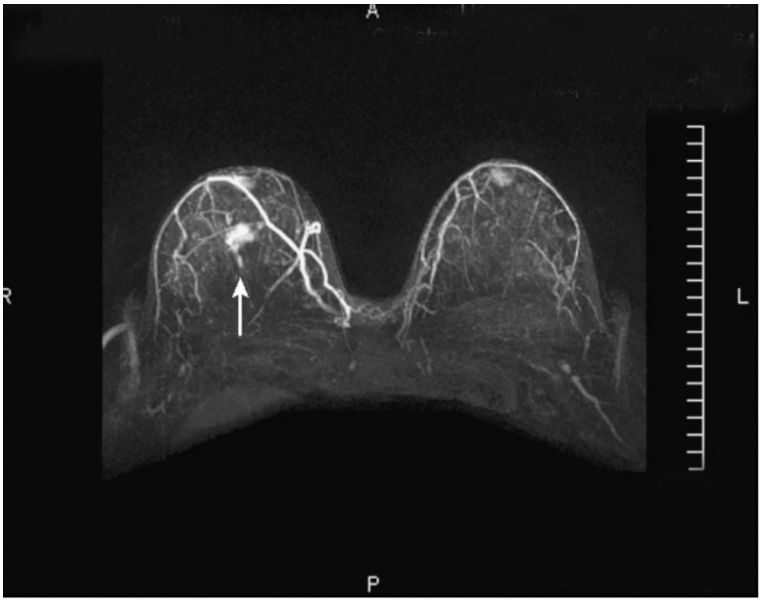

Below we show the line version of the previous lesion. This may then be a useful image process for analysis of a neural net input. The image reduction by line enhancement here actually allows for better clarification. It also presents an easier method to perform a pattern recognition.

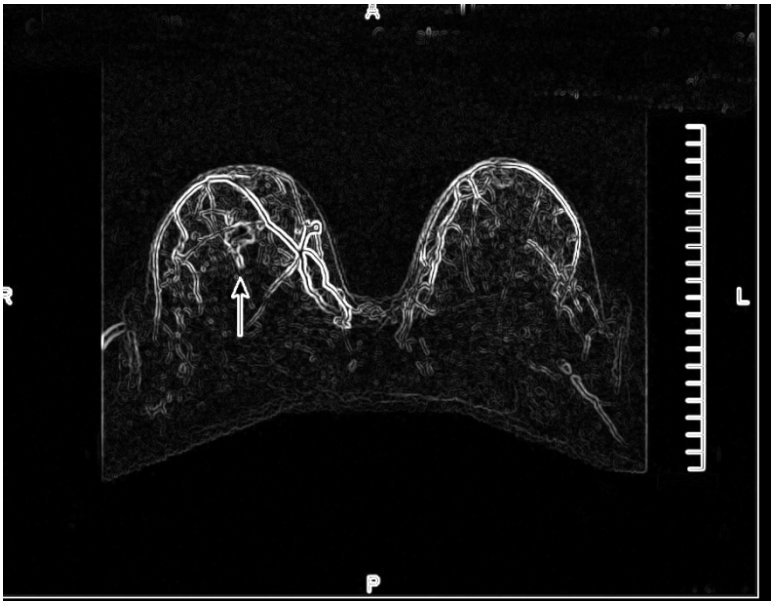

Now from Winfield et al we have a discussion integrating the biopsy with mpMRI:

In breast cancer, the addition of normalized ADCs to 3D T1-w and DCE-MRI data improves diagnostic performance (AUC 0.98 vs 0.89). The value of parameter combinations has been confirmed in other studies: analysis of 100 breast lesions (27 malignant and 73 benign) in 77 women showed that ADC is lower for lesions exhibiting predominantly washout or plateau

patterns than those exhibiting predominantly persistent enhancement, and in multivariate analysis, worst curve type and ADC were significant independent predictors of malignancy. Extension of mpMRI to 3 parameters (DCE-MRI, DW-MRI, and 3D 1H-MRSI) rather than 2 (DCE-MRI and DW-MRI) showed that the former yielded significantly higher areas under the curve than histology (0.936 vs 0.808) because of elimination of false negative lesions and reduction in false-positives.

Seven features derived from DW-MRI and DCE-MRI (e.g, slope, entropy, ADC) have been shown to discriminate malignant from benign lesions and their combination achieves the highest classification accuracy. The use of multiple parameters from DCE-MRI alone has illustrated the possibilities of identifying intrinsic imaging phenotypes of breast cancer based on hierarchical clustering of extracted feature vectors. These features have been linked to risk of recurrence based on gene expression.

5.2.4 Neural Nets

Neural nets have been examined in breast cancer diagnosis. As Sun et al have recently noted:

Breast cancer is the leading malignancy in females. Axillary lymph node (ALN) metastasis status is one of the most important factors in guiding treatment decision making in breast cancer. Traditionally, the nodal status was assessed by surgical methods such as sentinel lymph node biopsy (SLNB) and axillary lymph node dissection (ALND). According to the guideline from American Society of Clinical Oncology, SLNB is considered to have a high overall accuracy ranging from 93 to 97.6% with a relatively low false negative rate (FNR) ranging from 4.6 to 16.7% in detecting axillary metastasis. However, these surgical approaches have been considered controversial due to the invasiveness, potential complications, and possible overtreatment. Ultrasound is a widely-used tool in breast cancer assessment as it is non-invasive, radiation-free, real-time and well-tolerated in women.

Previous studies have shown that axillary ultrasound (AUS) may provide useful information relevant to ALN status in breast cancer. However, AUS alone has moderate sensitivity and may not be a reliable predictor for nodal metastasis. Recently, imaging-based machine learning approaches have been demonstrated promising in cancer diagnosis. There are two most popular machine learning approaches: radiomics analysis and convolutional neural networks (CNN). Radiomics analysis relies on a pipeline including extraction of numerous handcrafted imaging features, followed by feature selection and machine learning-based classification.

Handcrafted radiomics features extracted from the breast tumor area have been demonstrated predictive in ALN metastasis, with FNRs ranging from 13.9 to 25% (9, 10). However, handcrafted features are limited to the current knowledge of medical imaging, which may limit the potential of the predictive model. ***Deep learning improves this handcrafted pipeline by automatically learning discriminative features directly from images. Recent studies have shown that deep CNN-based approaches can achieve state-of-the-art performance in lesion detection and cancer diagnosis. To our knowledge, no studies have assessed breast ultrasound-based CNN in predicting ALN status for breast tumor****. Most studies have focused*

on mining predictive imaging features within the tumor, while the surrounding tissues were ignored.

Previous evidence has shown that the peritumoral region—the tumor-adjacent parenchyma immediately surrounding the tumor mass—may offer valuable outcome associated information. Two recent studies have demonstrated that handcrafted imaging features from peritumoral region in Dynamic Contrast-Enhanced MRI (DCE-MRI) are associated with sentinel lymph node metastasis and pathological complete response to neoadjuvant chemotherapy in breast cancer. Here, we hypothesize that deep CNN built based on intra- and peritumoral regions in breast ultrasound could provide relevant information in predicting ALN status. We are interested in comparing the performance of deep CNNs and radiomics models. Additionally, breast cancer can be classified into different molecular subtypes with distinct prognosis and respond differently to specific therapies.

Therefore, we further assessed if deep CNNs or radiomics models combining imaging features and molecular subtypes could offer improved accuracy. In this hypothesis-driven study, we first developed deep CNNs and radiomics models based on intratumoral, peritumoral, and combined regions in breast ultrasound images for predicting ALN metastasis. We then aimed to find out how on each region deep CNNs performed compared with radiomics models

We show a set of histology slides processed in the above manner. First the normal slide:

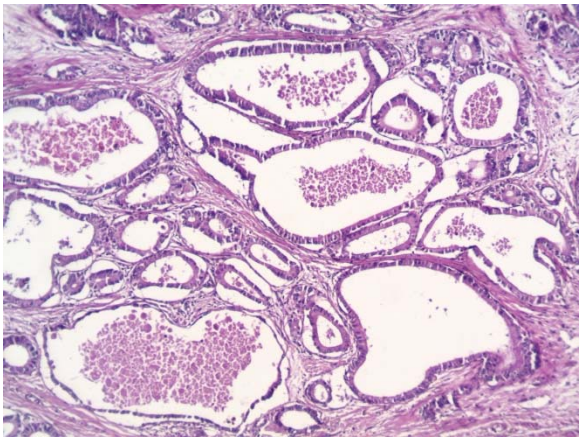

Second below is a closer examination of specific cells.

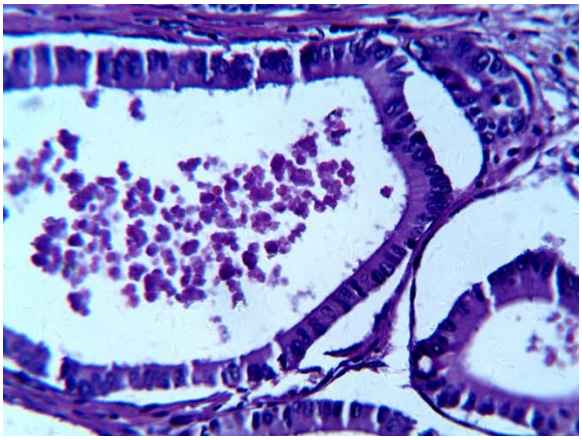

Third below is the above using a processed line analysis of the lesion. This makes for a much easier configuration of analyze.

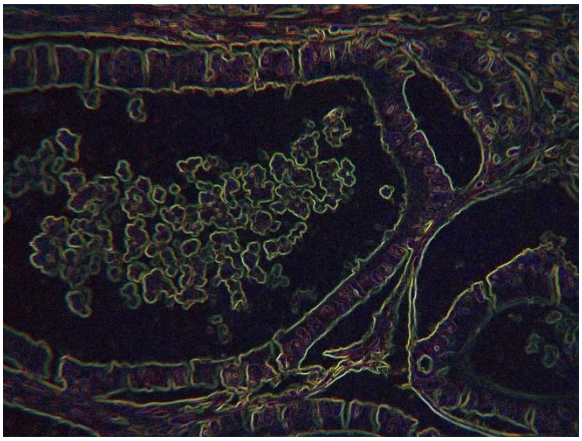

As Araujo et al have noted regarding convolutional neural networks on histological studies:

A CNN-based approach for the classification of H&E stained histological breast cancer images is proposed. All relevant features are learned by the network, reducing the need of field knowledge. Images are classified as either normal tissue, benign lesion, in situ carcinoma and invasive carcinoma. Alternatively, a binary classification as carcinoma or non-carcinoma is also performed. For this, the architecture of the network is designed to extract information from different relevant scales, including nuclei and overall tissue organization. The network is trained on an augmented patch dataset and tested on a separate set of images.

Both dataset augmentation and scale-based network design have been shown important for the success of the approach. The extracted features are also used for training a SVM classifier. Both CNN and SVM classifiers achieve comparable results. The proposed classification scheme allows to obtain high sensitivity for carcinoma cases, which is of interest for pathologists. The performance of our system is similar or superior to the state-of-the-art methods, even though a smaller and more challenging dataset is used. Finally, since the network is designed to consider

multiple biological scales, the proposed system can be extended for whole-slide breast histology image classification relevant for clinical settings.

The approach appears to function well on these types of cells. In a broader sense the work by Parekh et al note:

A new paradigm is beginning to emerge in Radiology with the advent of increased computational capabilities and algorithms. This has led to the ability of "real time" learning by computer systems of different lesion types to help the radiologist in defining disease. In particular using deep learning algorithms to segment and classify different radiological images. We chose to use multiparametric magnetic resonance imaging (mpMRI) parameters which capitalize on the different contrasts of tissue.

For example, using conventional and advanced MRI parameters of T1- and T2-weighted, diffusion weighted imaging (DWI) and dynamic contrast enhanced imaging (DCE) provide qualitative and quantitative information of different tissue types which can be used to construct "tissue" signatures information of tissue 1-4. Therefore, to integrate mpMRI and characterize breast tissue, we have developed a machine learning method coupled with deep learning for segmentation and characterization of breast tissue using mpMRI.

Deep learning networks (DLN) allow for the "learning" of radiological relationships between different tissue types and provides new methods to "segment" and/or classify high-dimensional data sets5-11. These DLN algorithms allow for accurate and reliable prediction of tissue types from "raw" input images with the aim to improve the radiologist's clinical decision support in different diseases12- 15 . Therefore, we implemented an unsupervised deep learning system based on stacked sparse autoencoders (SSAE). Autoencoders are unsupervised neural networks that are trained to create a compact or a low dimensional representation of its input via the hidden layer 7,9,16,17. The stacked sparse autoencoder network (SSAE) is a stack of sparse autoencoders with each autoencoder forming a layer of the SSAE.

This allows us to use deep learning to develop multiparametric breast tissue signatures across subjects, without prior knowledge of the lesion type for application to patients for tissue segmentation and classification of breast lesions…Utilizing multiparametric deep learning network, we have developed, tested, and validated a cognitive computing platform that organizes, integrates, and interprets imaging information using a MPDL tissue signature model. The application of the MPDL tissue signature model resulted in excellent segmentation and classification of different tissue classes.

This study employed an integrated multiparametric breast MRI deep learning model in the clinical setting and demonstrates that MPDL tissue signatures defines benign and malignant tissue and performs accurate classification. Moreover, this report demonstrates that deep learning-assisted unsupervised segmentation using mpMRI signatures can detect heterogeneous zones within breast lesions. These heterogeneous regions can be used for further classification of breast tissue by quantitative ADC maps and/or PK-DCE parameters. Finally, the MPDL model with machine learning classification distinguished between benign and malignant tissue with high sensitivity, specificity, and accuracy.

5.3 THYROID

Thyroid cancer is not as high and incidence as is many other cancers[21]. However with the expanded use of ultrasound the incidence is growing more rapidly than any other cancer. Yet the mortality has remained low. Most mortality from thyroid cancer is the result of advanced forms, especially anaplastic which is one of the most aggressive forms with near 100% mortality in three to six months. Thus thyroid cancer is a broadly defined malignancy. The question then is; how does one diagnose this form of cancer. We progress from ultrasound, through genomics and cytology. All present somewhat unique challenges and both ultrasound and cytology present challenging pattern recognition opportunities.

5.3.1 Ultrasound

The thyroid is near the surface of the body and is highly amenable to ultrasound examination. In fact US examination is the most cost effective diagnostic tool available. It is not dispositive of a malignancy but is highly suggestive. Below is a table of typical landmarks found in US scans.

Characteristic	*Sensitivity*	*Specificity*
Hypoechoic c/w surrounding thyroid	81% (48-90%)	53% (36-92%)
Marked hypoechogenicity c/w strap muscle	41% (27-59%)	94% (92-94%)
Microcalcifications	44% (26-73%)	89% (69-98%)
Macrocalcifications	10% (2-17%)	94% (84-98%)
Absence of halo	66% (33-100%)	43% (30-77%)
Irregular, microlobulated margins	55% (17-84%)	80% (62-85%)
Solid consistency	86% (78-91%)	48% (30-58%)
Taller-than-wide shape on transverse view	48% (33-84%)	92% (82-93%)

A typical US of a thyroid nodule is shown below evidencing many of the features consistent with a suspicious node.

[21] See: https://www.researchgate.net/publication/335404502_Thyroid_Cancer_and_Genetic_Differentiation , https://www.researchgate.net/publication/331935614_Thyroid_Cancer_Seek_and_Ye_Shall_Find

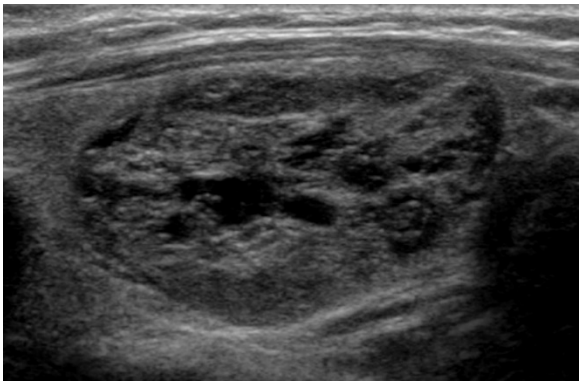

Statistically we can summarize these characteristics in the following chart.

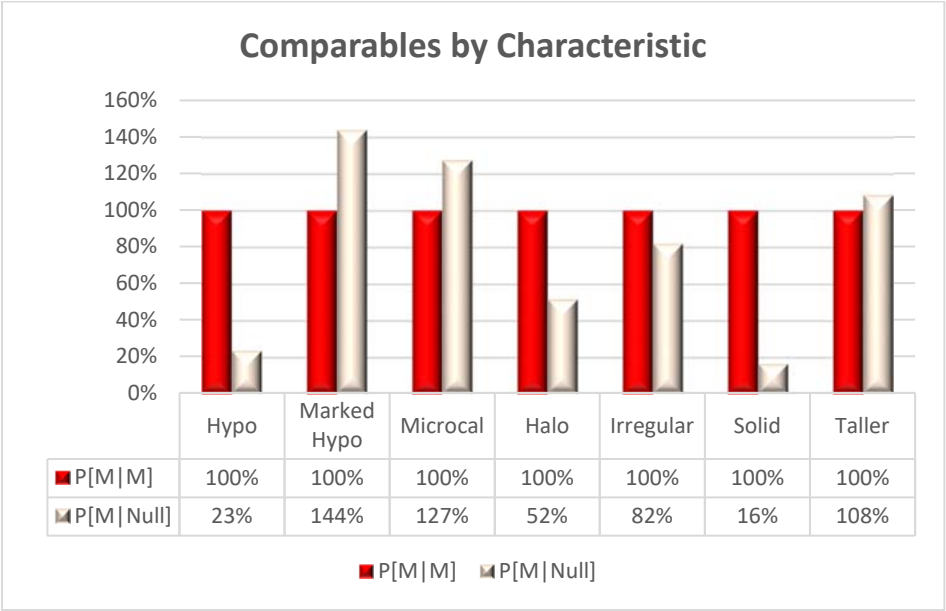

Note that we have normalized the ones where it is malignant to 100% to give the relative frequency to the same measure when there is no malignancy. We then plot the sensitivity and specificity below:

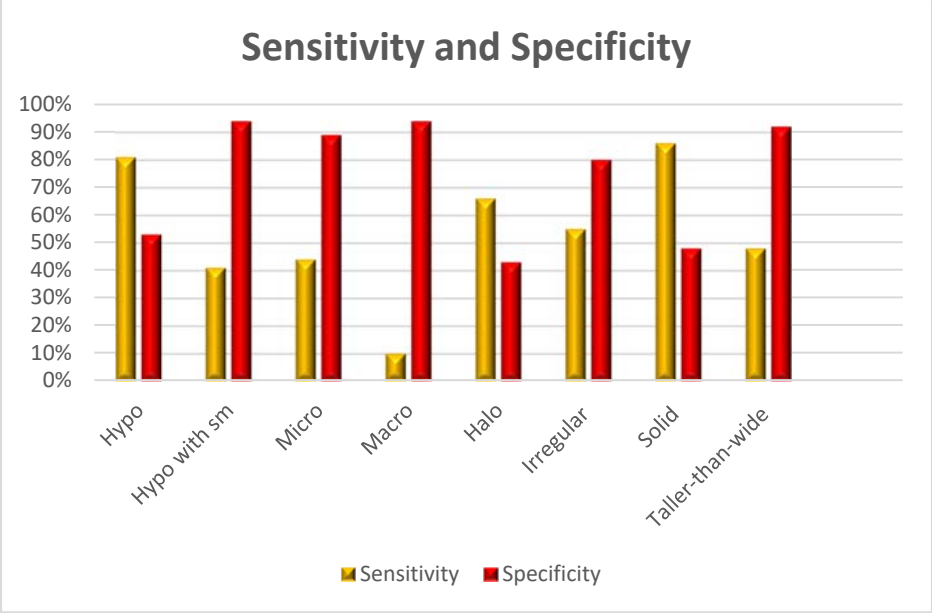

TI-RADS is the set of metrics which are used with thyroid US to assess if the lesion is suspicious. It is similar to the PI-RADS used in PCa. From Tessler et al, we have the following summary for TI-RADS:

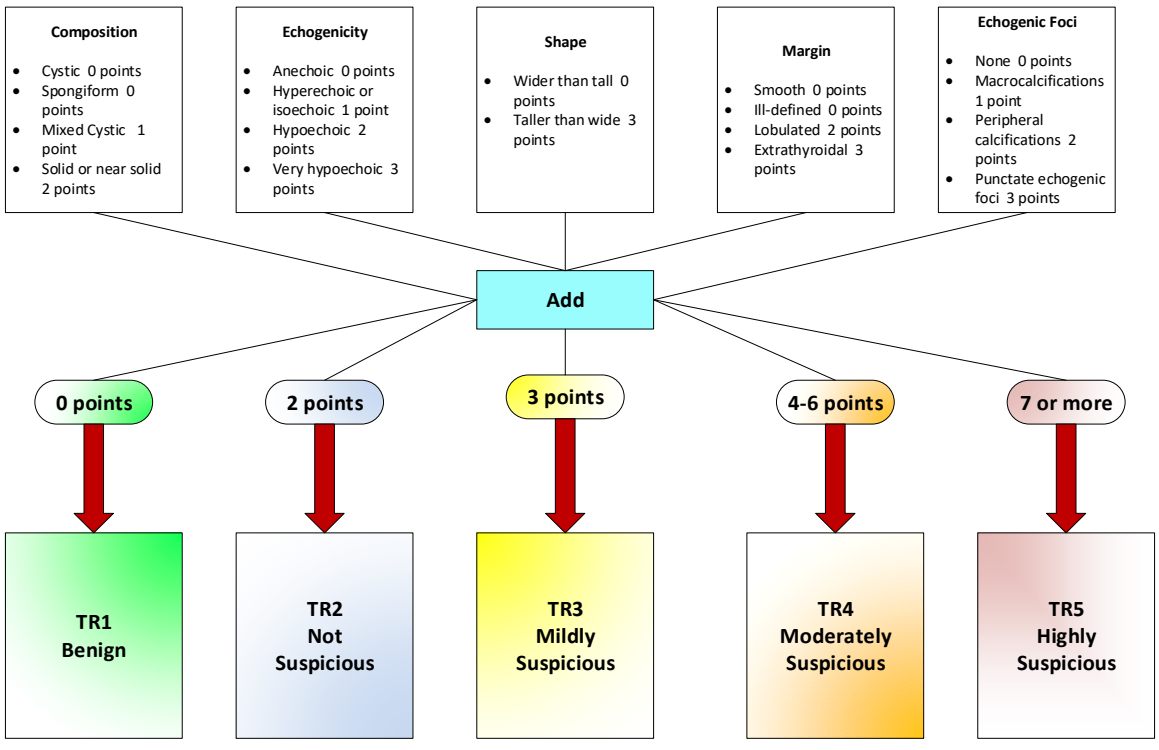

The following is a sample US analysis of a patient with multiple nodules. It yields a TR3 level. However it is also the case that when there are multiple nodules even at this level the risk of a malignancy is reduced.

Semantic feature	***Variations***	***Value***	***Nodule 1***	***Nodule 2***	***Nodule 3***
Size			***1.7 by 0.7 by 1.3***	***1.5 by 1.0 by 1.0***	***0.8 by 0.8 by 1.1***
			Right Upper	***Right Middle***	***Right Lower***
Composition					
	Solid	2			
	Predominantly Solid	1	1	1	1
	Predominantly Cystic	0			
	Cystic	0			
	Spongiform	0			
Echogenicity					
	Anechoic	0			
	Hyperechoic	1		1	1
	Isoechoic	1			
	Hypoechoic	2	2		
	Very hypoechoic	3			
Shape					
	Taller than wide	3			
	Wider than tall	0	0	0	0
Border					
	Smooth	0	0	0	0
	Irregular	2			
	Lobulated	2			
	Ill defined	0			
Halo					
	Present				
	Absent				
Extrathyroidal extension					
	Present	3			
	Absent	0	0	0	0

Semantic feature	*Variations*	*Value*	*Nodule 1*	*Nodule 2*	*Nodule 3*
Punctate echogenic foci					
	Present	3			
	Absent	0	0	0	
Macrocalcifications					
	Present	1			
	Absent	0			
Peripheral calcifications					
	Present	2			
	Absent	0			
Comet-tail artifacts					
	Present	0	0		
	Absent	0			
Score			**3**	**2**	**2**

Thus if we were to consider ways to automate these measurements we have multiple means and methods. For example let us consider two:

1. Pattern Recognition: In this approach we start with the identifying patterns as given. Then we must process the image to extract the patterns.

2. Neural Network: Let us assume a supervised neural network. Namely we assume we know the diagnosis and we have for each image a well-defined diagnosis. Then we may use a multilayer NN and have it trained so that when presented with a new US it can classify it as a score of say 1 to 7. The image is scanned via some form of convolutional NN, CNN, and based upon extensive training we can assess any unknown.

5.3.2 Genomic Analyses

A genomic analysis is not a radiomic test but it can be used in conjunction. However, radiomic tests in general, including histological and cytological are morphological and are in a sense reflective of the underlying genomic structure. Regrettably the linkage between morphology and genomics is still weakly understood and thus each reflects a somewhat orthogonal direction.

The following Table demonstrates the genomic profiles of various TCa.

			FA	HCA	NIFTP	FTC	HCC	PTC	PDTC	ATC	MTC[a]
Point mutations and indels		*BRAF* V600E, %					0	40-45	5-30	10-45	<5
		RAS, %	20-30	10-20	30-40	40-50	10-20	20	20-40	20-40	10-15
		EIF1AX, %	10-20	10-15	5-10	10-15	10-15	<5	10	10	
		PTEN, %	10-15		-5	10-15	10-15	<3	5-20	10-15	
		DICER1, %	10-15		-5	10-15		<5			
		7P53, %				<10	15-20	<5	10-30	50-70	<5
		TERT, %				15	10-20	5-10	30-50	70	
		PIK3CA, %	<5			<5		<5	5-20	5-18	
		AKT1, %							<5	<5	
		RET, %									40-50
Large-scale alterations	Fusions	*RET/PTC*, %						5-10	<5	<1	
		PPARG, %	5-10		20-30	10-20		<5	5-7	<1	
		NTRK1/3, %						<5	1-5		
		ALK, %						<5	5-10	<5	2
		THADA, %	5-10		20-30	<5		5			
		Somatic copy number alterations, %	20-40	40-50	20	40-50	70	5-10	50	90	20

5.3.3 Cytological Analyses

The third form of diagnostic analysis is cytological, both worth fine needle aspirations, FNA, and that of the excised tumor mass. The papillary form of TCa is interesting in that its diagnosis is a cellular diagnosis of specific forms and presentations. Unlike say PCa, where there is a proliferation of basal and or luminal cells, TCa has proliferation in the follicular form, and a papilla like growth in the papillary form, but the dispositive elements are those of how the cell appears, as we will show below.

Basically the thyroid cells is the outer side of a thyroid follicle. It is the boundary. This is shown below for a simple thyroid boundary. The cells on the boundary are well behaved and connected. Cell interfaces such as E-cadherin stabilize these cells. Internally to this glandular structure is a collagen internal fill. From this colloid under the pituitary control the T3 and T4 hormones are released. From this is the basis of the thyroid control path.

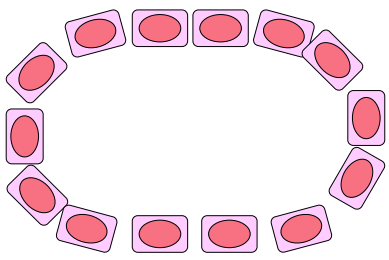

Now the thyroid gland is a compilation of these follicles as shown below. There are blood organs between the follicles and also C cells, cells separate from those that form the effective gland. The highly simplistic view is seen below.

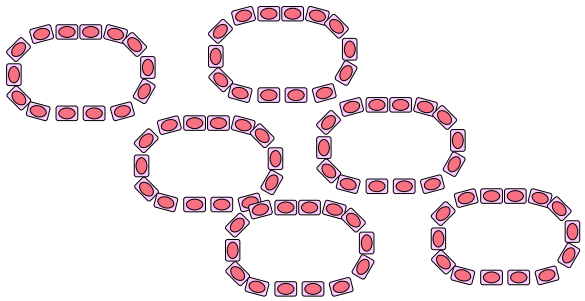

Inside is the collagen material used by the cells to produce T3 and T4.

The normal thyroid cells are shown below (From *Epstein, Biopsy Interpretation of the Thyroid*). The separate cells for enclosures which contain colloid and then it is processed and released by the cell. Surrounding the cell is and there are blood networks throughout the thyroid providing the cells with their requirements and transporting the cell products.

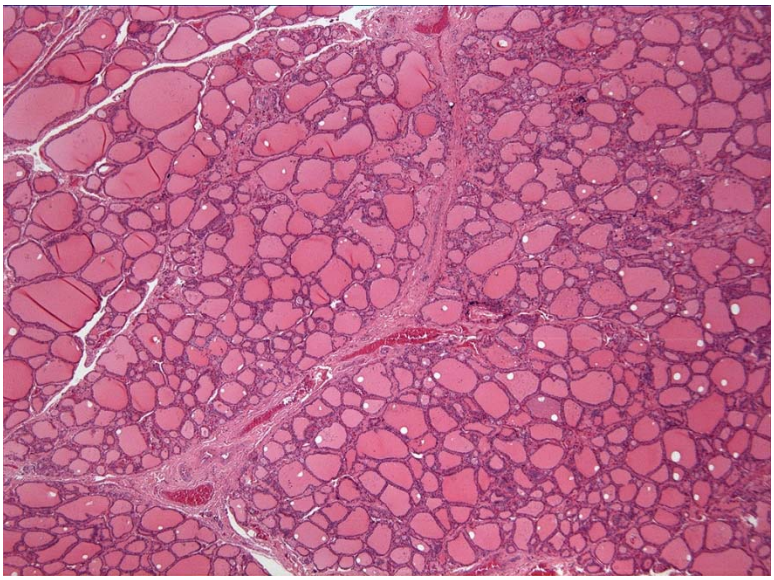

Further specific detail of a follicle is shown below (again from Epstein). Note the clarity and simplicity as well as structure of the cells in each small gland portion:

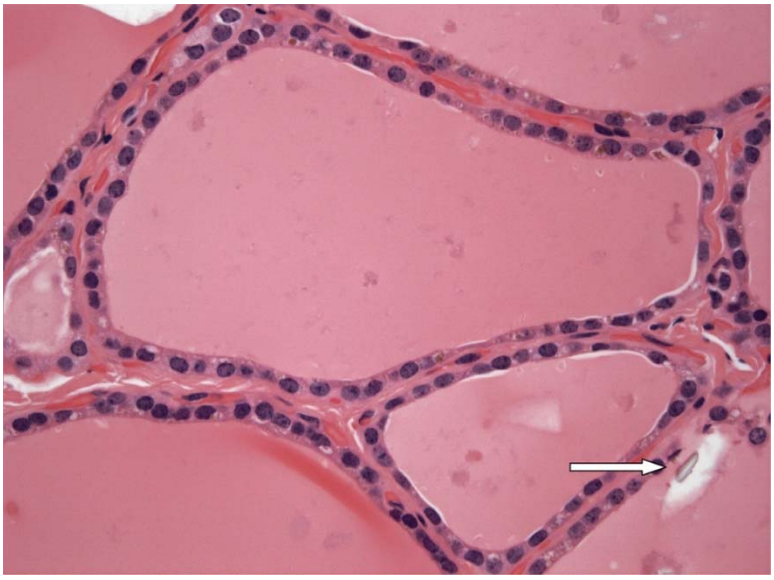

Note that the cells are well demarcated and organized. Now as we shall see, several variations occur as the cell becomes malignant. Growth results in a proliferation of cells, everywhere, loss of adhesion via EMT results in cell dislocation, and the morphology of individual cells change as well.

5.3.3.1 Papillary Growth

Now papilla are the small bumps or perturbances of the normal cells which generally are somewhat uniform as we have depicted.

The papillary like cells are shown as below:

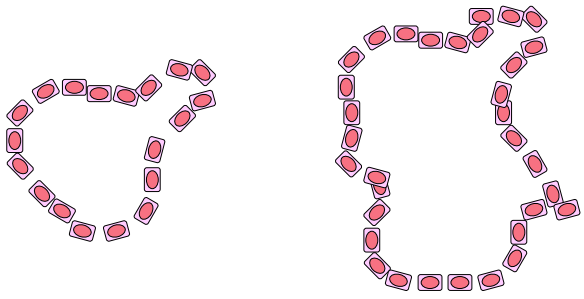

The above show the papilla, the bumps or offshoots. It can be argued that this papilla formation is a result of a quasi-EMT process where the E-cadherin bond structure is starting to deteriorate. Namely the genetic control of this is breaking down because of the suppression of the pathways that control epithelial like structure[22]. Now as Nucera and Pontecorvi have noted:

[22] See McGarty, EMT and Cancers, January 2019, https://www.researchgate.net/publication/330222973_EMT_and_Cancers

Most human thyroid cancers are differentiated papillary carcinomas (PTC). Papillary thyroid microcarcinomas (PTMC) are tumors that measure 1 cm or less. This class of small tumors has proven to be a very common clinical entity in endocrine diseases. PTMC may be present in 30-40% of human autopsies and is often identified incidentally in a thyroid removed for benign clinical nodules.

Although PTMC usually has an excellent long-term prognosis, it can metastasize to neck lymph nodes; however deaths related to this type of thyroid tumor are very rare. Few data exist on molecular pathways that play a role in PTMC development; however, two molecules have been shown to be associated with aggressive PTMC.

S100A4 (calcium-binding protein), which plays a role in angiogenesis, extracellular matrix remodeling, and tumor microenvironment, is over-expressed in metastatic PTMC. In addition, the BRAFV600E mutation, the most common genetic alteration in PTC, is present in many PTMC with extra thyroidal extension and lymph node metastasis.

The above observation is interesting. Namely that almost 40% of people will be harboring small PTCs which unless sampled by a good ultrasound examiner would never be found. Furthermore they would never grow. They also note regarding the papillary growth above:

BRAFV600E triggers a cascade that leads to human papillary thyroid microcarcinoma (PTMC) proliferation. The constitutive kinase activity of BRAFV600E phosphorylates and activates MEK1/2. Phospho-MEK1/2 induces hyperphosphorylation of ERK1/2 which translocates into the nucleus, triggering cell cycle progression, and abnormal cell proliferation by up-regulating cyclins (e.g., Cyclin D1) crucial for the checkpoint machinery in G1-S phases and inhibiting anti-cell cycle cyclins (e.g., p27). Up-regulation of cyclins (e.g., Cyclin D1) leads to hyper-proliferation of papillary thyroid microcarcinoma cells and increase in papillae size.

Now there are several additional and specific histological characteristics. For example, as Das notes[23]:

Psammoma bodies (PBs) are concentric lamellated calcified structures, observed most commonly in papillary thyroid carcinoma (PTC), meningioma, and papillary serous cystadenocarcinoma of ovary but have rarely been reported in other neoplasms and nonneoplastic lesions. PBs are said to represent a process of dystrophic calcification.

Despite numerous ancillary studies over a span of three and half decades, formation of PBs remains a poorly understood mechanism. Ultrastructural study of PTC has shown that thickening of the base lamina in vascular stalk of neoplastic papillae followed by thrombosis, calcification, and tumor cell necrosis leads to formation of PBs. Studies on serous

[23] Note: A psammoma body is a round collection of calcium, seen microscopically. The term is derived from the Greek word ψάμμος (psámmos), meaning "sand".

cystadenocarcinoma of ovary and meningioma, however, revealed that collagen production by neoplastic cells and subsequent calcification was responsible for the formation of PBs.

The existence of some precursor forms of PBs was reported in meningiomas and more recently in PTC, which were mostly in the form of extracellular hyaline globules surrounded by well-preserved neoplastic cells or in a smaller number of cases intracytoplasmic bodies liberated from intact tumor cells.

Cellular degeneration and necrosis, leading to the disappearance of neoplastic cells, were noticed by us only around PBs but not around the precursor forms. Based on the above findings, it is suggested that rather than being the outcome of dystrophic calcification of dead or dying tissue, PBs may indeed represent an active biologic process ultimately leading to degeneration/death of tumor cells and retardation of growth of the neoplasm. It may also serve as a barrier against the spread of neoplasm.

We show psammoma bodies below.

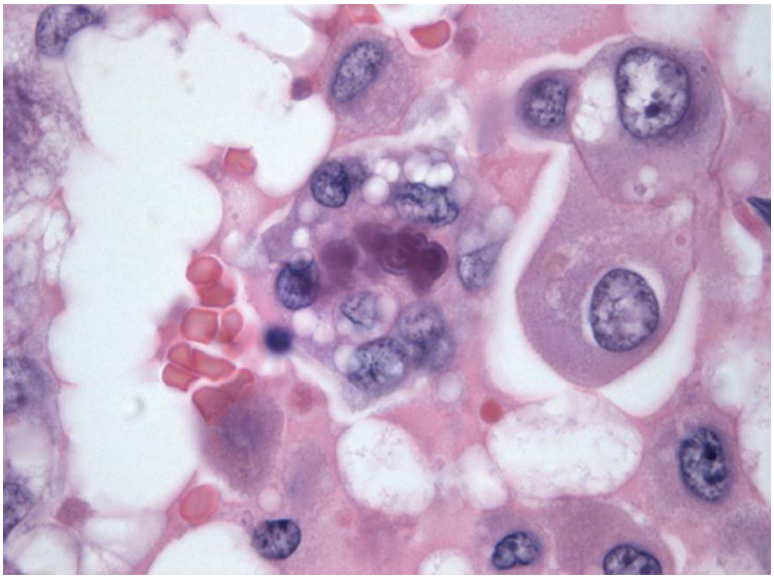

An additional example of specific histological characteristics is one with clear nuclei as shown below:

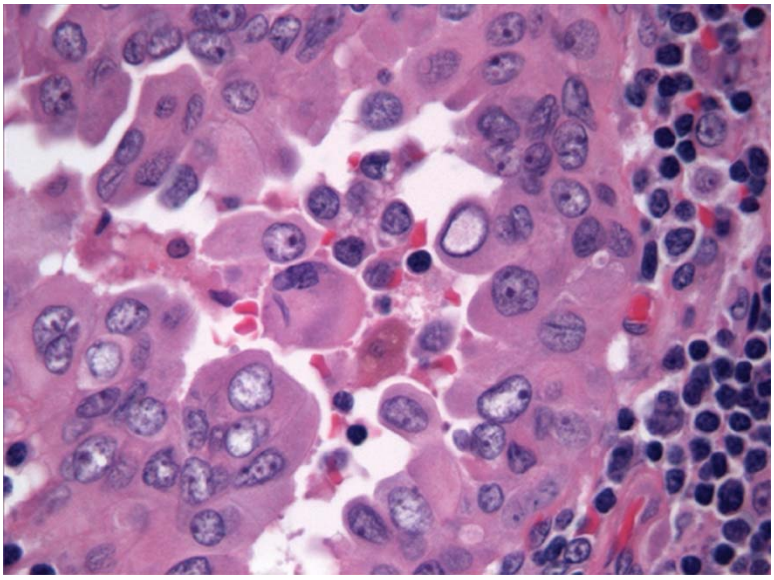

Another example of one type of papillary carcinoma is one with "Orphan Annie" eyes, the wide open white eyes of the nucleus in the cells below.

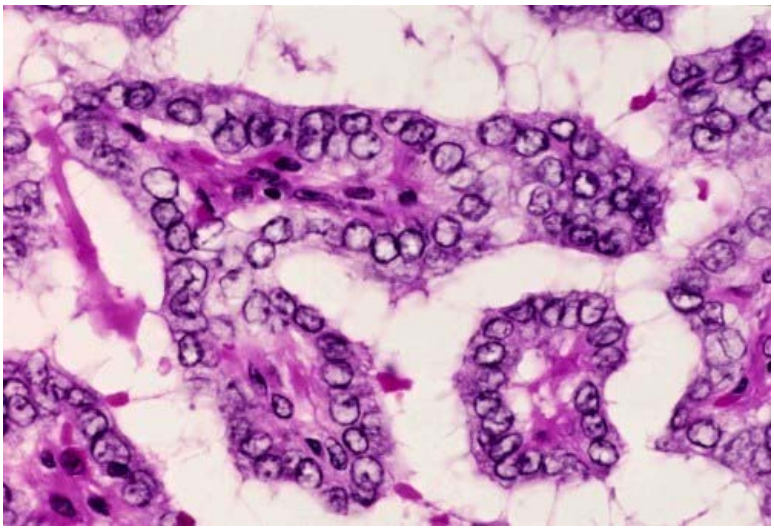

Note also the well demarcated papillary form with outstretches of the otherwise well-structured cell.

Finally an added one is cells with nuclear grooves is a characteristic that is part of this diagnosis as shown below:

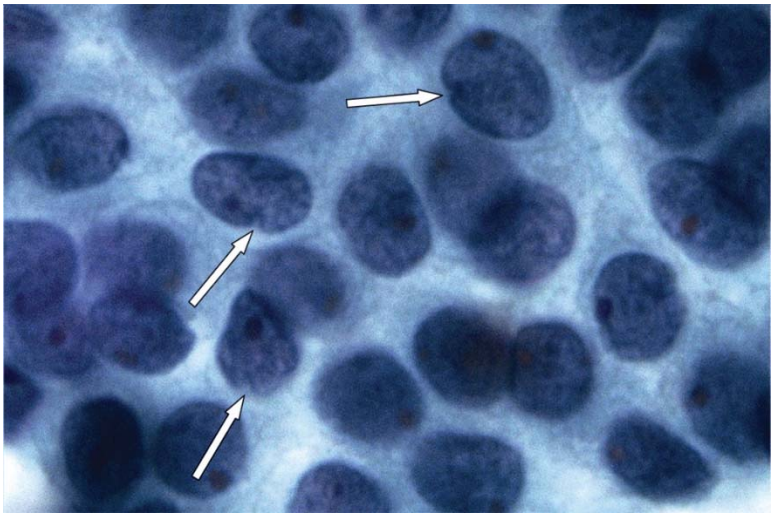

These are small notches seen in the side of the nucleus.

Now these are what a trained histopathologist would be looking for. However, an underlying question is; why are they present and what causes these specific characteristics. We frequently see in medicine the answers to what but not why. Some of these answers are yet to be determined.

5.3.3.2 Follicular Growth

In contrast to follicular carcinoma, where the boundary patency gets deformed, follicular carcinoma is where there is a proliferation of the follicular cells.

Baloch and LiVolsi have noted:

Follicular carcinoma comprises about 5% of thyroid cancers; however, in iodide-deficient areas, this tumor is more prevalent making up 25-40% of thyroid cancers. The true incidence of follicular carcinoma is difficult to determine since the follicular variant of papillary carcinoma may still be placed into this category. Risk factors include iodine deficiency, older age, female gender, and radiation exposure (although the relationship of radiation to follicular carcinoma is far less strong than with papillary cancer).

Clinically, follicular carcinoma usually presents as a solitary mass in the thyroid. Follicular carcinoma has a marked propensity for vascular invasion and avoids lymphatics; hence, true embolic lymph node metastases are exceedingly rare. Follicular carcinoma disseminates hematogenously and metastasizes to bone, lungs, brain, and liver …

What are the minimum criteria for making this diagnosis? Invasion of the capsule, invasion through the capsule, and invasion into veins in or beyond the capsule represent the diagnostic criteria for carcinoma in a follicular thyroid neoplasm. The criterion for vascular invasion applies solely and strictly to veins in or beyond the capsule, whereas, the definition of capsular invasion is controversial. Some authors require penetration of the capsule to diagnose a

follicular tumor as carcinoma, while others need tumor invasion through the capsule into the surrounding normal thyroid.

Is capsular invasion insufficient for the diagnosis of follicular cancer? Distant metastases have been reported in follicular carcinoma diagnosed only on the basis of capsular and not vascular invasion, however, in some cases, metastases were already present at initial diagnosis. The presence of vascular invasion is also indicative of malignancy in a follicular tumor. Invasion of vessels within or beyond the lesional capsule is necessary for a definitive diagnosis of vascular invasion. The lesions with vascular invasion should be separated from the minimally invasive follicular carcinomas that show capsular invasion only, because angio-invasive lesions have a greater probability of recurrence and metastasis.

Thus a simplistic view of a follicular cancer is shown below.

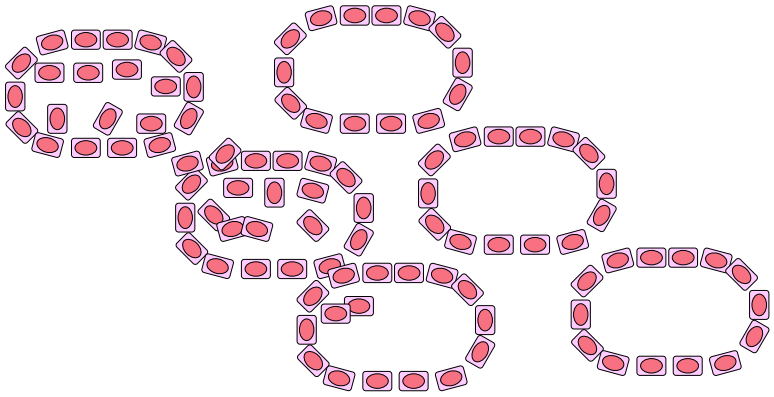

We depict a follicular cancer below:

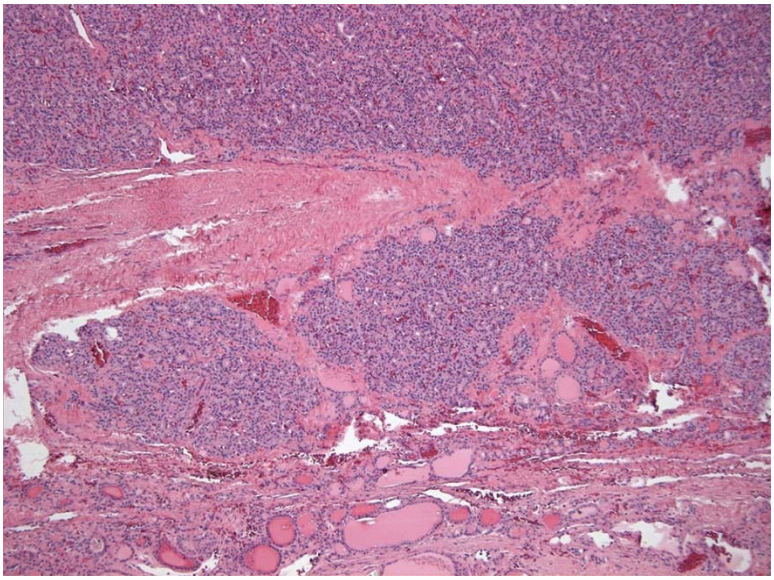

This shows the multiplicity of cells in what was initially a well ordered cell structure filled with collagen.

Note the extensive infiltration. Again in simplistic terms, papillary is a form where we lose shape, namely a putative EMT transition and follicular is where we see extensive proliferation. Clearly both forms may occur.

5.3.3.3 Neuroendocrine Growth and Medullary Thyroid Cancer

Medullary thyroid cancer is basically a neuroendocrine cancer. Neuroendocrine cancers are an interesting subset of many cancers and it worth reviewing the overall paradigm of their growth.

Namely we look at neuroendocrine type effects and thus it requires a slightly more detailed understanding of the prostate As NCI notes[24]:

Neuroendocrine: Having to do with the interactions between the nervous system and the endocrine system. Neuroendocrine describes certain cells that release hormones into the blood in response to stimulation of the nervous system.

We then, in a rationalistic manner, can try and connect the other empirical facts and see if the initial observation can also be logically correct and from that logic ascertain a new therapeutic approach.

A simplistic view of a neuroendocrine system is shown below. Basically the neuro cell activates the endocrine cell which in turn sends out signals to other collections of cells to do whatever they are supposed to do.

[24] https://www.cancer.gov/publications/dictionaries/cancer-terms/def/neuroendocrine

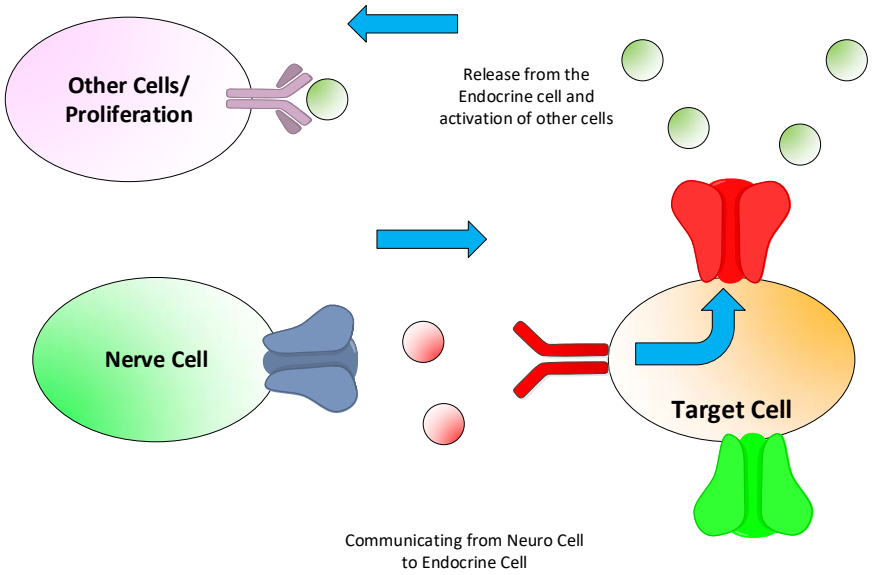

The above is simplistic but based upon a substantial base of validated cellular signalling factors. Namely these results are empirical in a broad sense. Now when examining various cancers we often look at the cancer cell as being the driving factor. However in a neuroendocrine environment, the cancer cell may be getting its signalling from a cancer initiating cell which in turn is being signaled by a neuro cell. The cancer initiating cell may be blocked by blocking the signalling between it and the causative neuro cell. That is the logical or rationalistic part of this exercise.

The questions now are;

(i) If the malignancy occurs in the neuroendocrine cell, then does it create an environment for proliferation of other cells?

(ii) If the malignancy occurs in the neuroendocrine cell does it send out signals that either block other homeostatic processes or does it accelerate angiogenesis in the new malignancy?

(iii) If the malignancy starts in a non-neuroendocrine cell, are there processes that effectively "turn on" the neuroendocrine cell to facilitate such effects as proliferation, angiogenesis, gene suppression or activation in other cells?

These are but a few of the questions which may be posed. Again we indicate that this is a bit simplistic but it does present the key issues related hereto.

We have examined neuroendocrine driven cancers when examining the prostate. They are simply cancers where a local neuroendocrine cell starts controlling the proliferation process.

As Franz notes:

Medullary thyroid cancer (MTC) is a tumor of the parafollicular C cells that accounts for approximately 10% of all thyroid malignancies. An estimated 75% of MTC cases are sporadic, and the remaining 25% are familial. Embryologically, these cells originate within the neural crest and function similarly to other neuroendocrine cells within the amine precursor uptake and decarboxylation system.

C cells are distributed throughout the entire thyroid gland, although they tend to predominate in the upper poles. Calcitonin, a hormone active in calcium metabolism, is synthesized and secreted by C cells and therefore serves as a useful serum marker for the presence of MTC. Calcitonin levels are most useful in screening individuals who are genetically predisposed to the disease and in following patients who already have been treated. The recent identification of the gene responsible for heritable forms of MTC has allowed earlier identification of individuals at risk for the disease

Kim and Kuo have noted:

Medullary thyroid carcinoma (MTC) is a rare neuroendocrine tumor derived from the thyroid C cells producing calcitonin. MTC accounts for 0.6% of all thyroid cancers and incidence of MTC increased steadily between 1997 and 2011 in Korea. It occurs either sporadically or in a hereditary form based on germline rearranged during transfection (RET) mutations. MTC can be cured only by complete resection of the thyroid tumor and any loco-regional metastases.

The most appropriate treatment is still less clear in patients with residual or recurrent disease after initial surgery or those with distant metastases because most patients even with metastatic disease have indolent courses with slow progression for several years and MTC is not responsive to either radioactive iodine therapy or thyroid-stimulating hormone suppression. Recently, two tyrosine kinase inhibitors (TKIs), vandetanib and cabozantinib, are approved for use in patients with advanced, metastatic or progressive MTC.

Baloch and LiVolsi note:

Medullary thyroid carcinoma comprises less than 10% of all thyroid malignancies. This tumor is of great diagnostic importance because of its aggressiveness, its close association with multiple endocrine neoplasia syndromes (MEN2A and 2B), and a relationship to a C cell hyperplasia, a probable pre cursor lesion.

While the majority of medullary carcinomas are sporadic, about 10-20% are familial. Since these familial cases have been identified, a gene associated with medullary carcinoma has been identified on chromosome 10 and involves mutations in the RET oncogene.

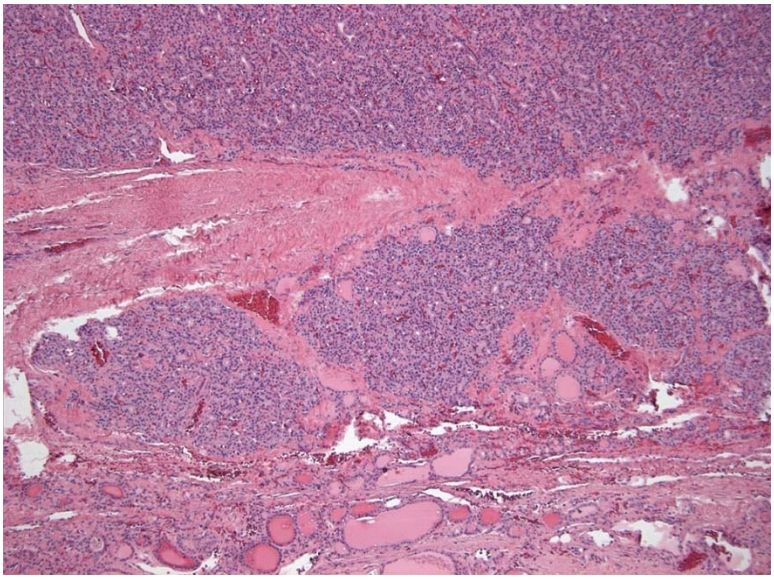

and below:

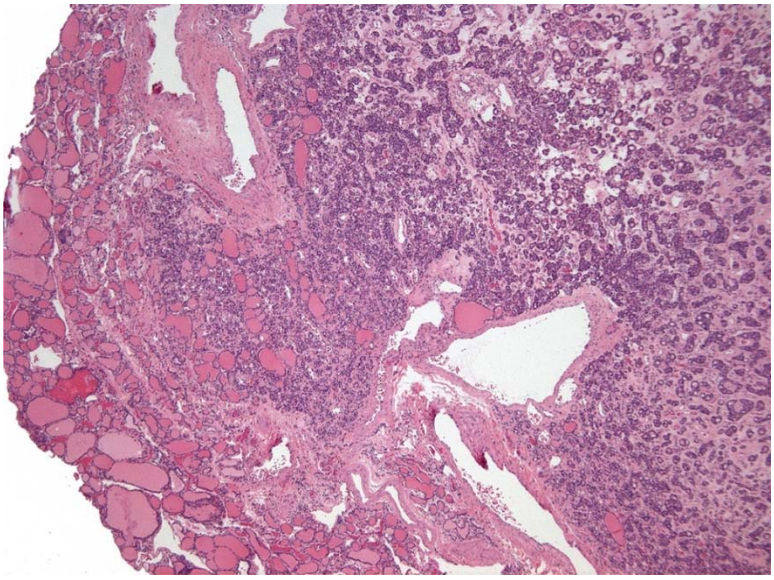

5.3.3.4 Anaplastic

This is a highly aggressive cancer with nearly 100% mortality in 6 to 12 months. It is also quite rare but seems to be a sequella to a Graves diseased thyroid. Given its rarity and complexity it is worth just a mention.

5.3.4 Expert Systems

As Chamrara and Ying have note for CADS systems:

This review suggests that CAD of thyroid ultrasound features has a good diagnostic performance which is comparable to that of radiologists' qualitative assessment with the potential for improved overall diagnostic accuracy when qualitative and quantitative approaches are combined. The nodule size, the experience of the operator and the choice of TIRADS system are potential influencers of CAD diagnostic performance. Future multi-center studies that compare similar CAD software based on standardized approaches and assess the diagnostic performance of combined Doppler ultrasound CAD and grey scale ultrasound CAD of the same thyroid nodules are recommended to further evaluate the clinical role of CAD in thyroid nodule characterization.

5.4 SUMMARY

In the examples above we considered imaging studies such as CAT, US, mpMRI amongst many and also histological and cytological studies. We considered pattern recognition approaches which use standard metrics such as PI-RADS and TI-RADS and histological and cytological metrics as well. We summarize some of these below.

Cancer	*Imaging*	*Cyto/Histo*
Prostate	mpMRI for measurement of putative lesion areas using DW approaches as well as DCE, Then use of integrated and correlated US and mpMRI	Primarily histological demonstrating loss of acinar structure and proliferation of basal cells. Loss of form and graduated pleiomorphic structure.
Colon	CAT or MRI looking for polyps	Loss of papillary structure
Breast	X ray or mpMRI looking for lesions.	Loss of glandular structure
Thyroid	Ultrasound metrics such as	Cytological markers such as irregular borders of nucleus, clear nucleus, orphan Annie eyes etc.

6 OBSERVATIONS

Based upon the above presentation we now consider several observations.

6.1 RNA MARKERS

As Demster et al have noted,

Is it the gene or the expression of the gene? Is it the DNA or the RNA? As we progress in understanding cancers we often look for the putative gene. DNA can be read and the presence of absence of the gene is considered dispositive. However, it often is not.

The real if is; does the gene do anything? Namely does it produce an RNA and in turn a protein? In a recent paper Biorxiv, CSHL, we have an interesting result. The authors note:

Disappointing results with genome-based biomarkers have driven calls to look beyond the cancer genome to other possible indicators of cancer-specific vulnerabilities. A major alternative for tumor characterization is the transcriptome. Although RNA is more difficult to maintain in the clinic than DNA, studies have found that gene expression supplies the most significant predictive features for patient prognosis6. Previous work on predicting cell viability after compound treatment suggests that expression may be more powerful than DNA features for predicting drug response, but expression-based models are widely treated as undesirable either because they are considered trivial proxies for tissue-type or because they are seen as uninterpretable9. These suggestive studies point to the need for a comprehensive comparison of expression and genomic molecular features as predictors of cancer vulnerability and a deeper interrogation of the interpretability of expression models.

Here we present the first such study across five large datasets of cancer cell viability including both genetic and chemical perturbations. We find that RNA-Seq expression outperforms DNA-derived features in predicting cell viability response in nearly all cases, including many perturbations with known genomic biomarkers. The best results are typically driven by a small number of interpretable expression features. Our findings suggest that both existing and new cancer targets are frequently better identified using RNA-seq gene expression than any combination of other cancer cell properties.

RNA can be fragile and more difficult to assess. We have seen that RNA-seq does provide a means and have seen this in miRNA analyses. Perhaps this is an added methodology worthy of pursuit.

6.2 NEURAL NETWORKS AND DIMENSIONALITY

I am wary of neural nets. As an example of this concern a recent paper by Poggio et al discusses some the issues as follows:

Once upon a time, models needed more data than parameters to provide a meaningful seem to avoid this basic constraint. In fact, more weights fitting. Deep networks than data is the standard situation for deep-learning networks that typically fit the data and still show good predictive performance on new data1. Of course, it has been known for some time that the key to good predictive performance is controlling the complexity of the network and not simply the raw number of its parameters.

The complexity of the network depends on appropriate measures of complexity of the space of functions realized by the network such as VC dimension, covering numbers and Rademacher numbers. Complexity can be controlled during optimization by imposing a constraint, often under the form of a regularization penalty, on the norm of the weights, as all the notions of complexity listed above depend on it. The problem is that there is no obvious control of complexity in the training of deep networks! This has given an aura of magic to deep learning and has contributed to the belief that classical learning theory does not hold for deep networks

What Poggio is saying is that if we want to find a and b in the following:

y=ax+b

then we often have lots of x and y values. In deep learning neural nets, say an image, we may have lots of as and bs and few x and y. That makes for an exceptionally unstable situation, in fact it is often if not always an indeterminate one! Yet using a neural network one would never know that! They always give answers, like those machines at amusement parks always giving a fortune.

Thus the deep learning or neural nets was have examined may putatively have unstable end points.

6.3 SPEECH RECOGNITION TO IMAGE RECOGNITION

There is a bit of a parallel between the progress in speech recognition and in turn our discussion of image recognition. Speech recognition took over seventy years of work. Understanding human speech, understanding linguists and so forth. Neural nets seem to work quite well. However the effort was monumental. Now image recognition may follow a similar path yet it is significantly more complex.

7 REFERENCES

1. Aggarwal, Neural Networks and Deep Learning, Springer, 2018
2. Ahdoot et al, MRI-Targeted, Systematic, and Combined Biopsy for Prostate Cancer Diagnosis, NEJM, 382;10, March 5, 2020
3. Araujo et al, Classification of breast cancer histology images using Convolutional Neural Networks, PLOS ONE, June 1, 2017
4. Bagheri et al, Advances in medical imaging for the diagnosis and management of common genitourinary cancers, Urol Oncol. 2017 July; 35(7): 473–491
5. Bagheri et al, Advances in medical imaging for the diagnosis and management of common genitourinary cancers, Urol Oncol. 2017 July; 35: 473–491
6. Bard et al, Image Guided Prostate Cancer Treatments, Springer, 2014
7. Bard et al, Image Guided Prostate Cancer Treatments, Springer, 2014
8. Bargaje et al, Review of Classification algorithms for Brain MRI images, International Research Journal of Engineering and Technology (IRJET), Volume: 04 Issue: 01 | Jan-2017
9. Barrett, What is multiparametric-MRI of the prostate and why do we need it?, Imaging Med. (2015) 7
10. Bax et al, Review and Comparison of Cancer Biomarker Trends in Urine as a Basis for New Diagnostic Pathways, Cancers 2019, 11, 1244
11. Berens et al, Multiscale, multimodal analysis of tumor heterogeneity in IDH1 mutant vs wild-type diffuse gliomas, PLOS ONE 14(12): e0219724, 2019
12. Birkfeliner, Applied Medical Image Processing, CRC, 2011
13. Boerer and Asa, Biopsy Interpretation of the Thyroid, 2nd Ed, Wolters Kluwer, 2017
14. Braman et al, Association of Peritumoral Radiomics With Tumor Biology and Pathologic Response to Preoperative Targeted Therapy for HER2 (ERBB2)–Positive Breast Cancer, JAMA Network OPEN, 2019
15. Brezinski, Optical Coherence Tomography, Academic, 2016
16. Brown and Semelka, MRI Basics, Principles and Applications, Wiley, 2003.
17. Bryant et al, Predicting High-Grade Cancer at Ten-Core Prostate Biopsy Using Four Kallikrein Markers Measured in Blood in the ProtecT Study, JNCI J Natl Cancer Inst (2015) 107(7)
18. Bushberg et al, The Essential Physics of Medical Imaging, Wolters, 3rd Ed, 2012
19. Campanella et al, Quantification of cancer risk of each clinical and ultrasonographic suspicious feature of thyroid nodules: a systematic review and meta-analysis, Bioscientifica, 2014

20. Cantley ey al, Signal Transduction, CSHL Press, 2014
21. Chambara and Ying, The Diagnostic Efficiency of Ultrasound Computer–Aided Diagnosis in Differentiating Thyroid Nodules: A Systematic Review and Narrative Synthesis, Cancers 2019, 11, 1759
22. Cheon and Lee, Color Edge Detection based on Bhattacharyya Distance, Proceedings of the 14th International Conference on Informatics in Control, Automation and Robotics (ICINCO 2017) - Volume 2, pages 368-371
23. Cover and Hart, Nearest Neighbor Pattern Classification, IEEE Info Theory, Jan 1967
24. Custem, Imaging in Colorectal Cancer: Progress and Challenges for the Clinicians, Cancers 2016, 8, 81
25. Decazes and Bohn, Immunotherapy by Immune Checkpoint Inhibitors and Nuclear Medicine Imaging: Current and Future Applications, Cancers 2020, 12, 371
26. Demster et al, Gene expression has more power for predicting in vitro cancer cell vulnerabilities than genomics, https://www.biorxiv.org/content/10.1101/2020.02.21.959627v1
27. Devi et al, Detection of Cervical Cancer using the Image Classification Algorithms, IJCTA, 9(3), 2016, pp. 153-166
28. Dhawan, Medical Image Analysis, IEEE, 2011
29. Duda and Hart, Pattern Classification and Scene Analysis, Wiley, 1973
30. Duick et al, Thyroid and Parathyroid Ultrasound and Ultrasound Guided FNA, 4th Ed, Springer, 2018
31. Eiber et al, Prostate Cancer Molecular Imaging Standardized Evaluation (PROMISE): Proposed miTNM Classification for the Interpretation of PSMA-Ligand PET/CT, The Journal of Nuclear Medicine • Vol. 59 • No. 3 • March 2018
32. Eisenhauer et al, New response evaluation criteria in solid tumours: Revised RECIST guideline, European Journal of Cancer 45 (2009) 228 – 247
33. Epstein, Biopsy Interpretation of the Prostate, 6th Ed, Wolters Kluwer, 2020
34. Fan et al, Radiomic analysis reveals DCE-MRI features for prediction of molecular subtypes of breast cancer, PLOS One, Feb 6, 2017
35. Fehr, et al, Automatic classification of prostate cancer Gleason scores from multiparametric magnetic resonance images, PNAS Nov 2, 2015
36. Friedman et al, Principles of MRI, McGraw Hill, 1989.
37. Fukunaga, Introduction to Statistical Pattern Recognition, Academic, 2nd Ed, 1990
38. Galimzianova et al, Toward Automated Pre-Biopsy Thyroid Cancer Risk Estimation in Ultrasound,
39. Gartner and Hiatt, Textbook of Histology, 3rd Ed, Saunders 2006
40. Gearhart and Ahuja, Colorectal Cancer, Saunders, 2011

41. Ghai and Haider, Multiparametric-MRI in diagnosis of prostate cancer, Ind Jrl Uro, 2015, Vol 31, Issue 3
42. Ghai and Haider, Multiparametric-MRI in diagnosis of prostate cancer, Indian J Urol. 2015 Jul-Sep; 31: 194–201
43. Goldman and Schafer, Goldman's Cecil Medicine, 24th Ed, Elsevier, 2012
44. Gonzalez and Woods, Digital Image Processing, 4th Ed, Pearson, 2018
45. Guorong et al, Bhattacharyya Distance Feature Selection, Proceedings of the 13th International Conference on Pattern Recognition, vol. 2, pp. 195-199, 1996
46. Gurusamy and Subramaniam, A Machine Learning Approach for MRI Brain Tumor Classification, CMC, vol.53, no.2, pp.91-108, 2017
47. Halicek et al, Deep convolutional neural networks for classifying head and neck cancer using hyperspectral imaging, J. Biomed. Opt. 22(6), 060503 (2017)
48. Hariharan, Optical Interferometry, Academic, 2003
49. Hasan et al, Segmentation of Brain Tumors in MRI Images Using Three-Dimensional Active Contour without Edge, Symmetry 2016, 8, 132
50. Haykin, Neural Networks, 3rd Ed, Pearson, 2016
51. Horowitz, MRI Physics for Physicians, Springer, 1989
52. Huettel et al, Functional Magnetic Resonance Imaging, Sinauer, 2009.
53. Jacobs and Finlayson, Breast Cancer, Saunders, 2011
54. Jain et al, Statistical Pattern Recognition: A Review, IEEE Transactions On Pattern Analysis And Machine Intelligence, Vol. 22, No. 1, January 2000
55. Jelinek, Statistical Methods for Speech Recognition, MIT Press, 1997
56. Jurafsky and Martin, Speech and Language Processing, Prentice Hall, 2000
57. Kak and Slaney, Computerized Tomographic Imaging, IEEE, 1988
58. Karp and Falchook, Targeted Cancer Therapy and Immunotherapy, 2nd Ed, Wolters Kluwer, 2019
59. Korn, A Multiparametric MRI for the Classification and Grading of Prostate Cancer, UCSF PhD Thesis, 2019
60. Kuhl et al, Mammography, Breast Ultrasound, and Magnetic Resonance Imaging for Surveillance of Women at High Familial Risk for Breast Cancer, Jrnl Clin Onc, Nov 2005
61. Kuhl, The Changing World of Breast Cancer, Investigative Radiology • Volume 50, Number 9, September 2015
62. Kumar et al, Basic Pathology, Elsevier, 2018
63. Kumar et al, QIN "Radiomics: The Process and the Challenges", Magn Reson Imaging. 2012 November; 30: 1234–1248

64. Larrea et al, New Concepts in Cancer Biomarkers: Circulating miRNAs in Liquid Biopsies, Int. J. Mol. Sci. 2016, 17, 627

65. Li e al, Robust Automatic Speech Recognition, Academic, 2016

66. Liang and Lauterbur, Principles of Magnetic Resonance Imaging, IEEE Press, 2000.

67. Long and Wong, The Chemistry of Molecular Imaging, Wiley, 2015

68. Lufkin, The MRI Manual, Year Book Med Pub, 1990

69. McGarty: Cancer Immunotherapy: A Systems Approach. 03/2017; Telmarc.

70. McGarty: Health Care Policy. 08/2009; DRAFT.

71. McGarty: Hemerocallis: Species, Hybrids and Genetics. 10/2009; , DOI:10.13140/2.1.1921.9843

72. McGarty: Melanoma Genomics. 06/2012; TBD., DOI:10.13140/2.1.1426.6242

73. McGarty: Prostate Cancer: A Systems Approach. 10/2012; TBD., DOI:10.13140/2.1.2475.2007

74. McGarty: Stochastic Systems and State Estimation. 06/1974; Wiley.

75. McRobbie et al, MRI, From Picture to Proton, Cambridge, 2003.

76. Minsky and Papert, Perceptrons, MIT Press, 1969

77. Monti et al, Multiparametric MRI for Prostate Cancer Detection: New Insights into the Combined Use of a Radiomic Approach with Advanced Acquisition Protocol, Cancers 2020, 12, 390

78. Motlak, Detection and Classification of Breast Cancer Based-On Terahertz Imaging Technique Using Artificial Neural Network & K-Nearest Neighbor Algorithm, International Journal of Applied Engineering Research ISSN 0973-4562 Volume 12, Number 21 (2017) pp. 10661-10668

79. Murphy et al, The Expanding Role of MRI in Prostate Cancer. Gen Imag, AJR, V 201, Dec 2013

80. Nie et al, Rectal Cancer: Assessment of Neoadjuvant Chemo-Radiation Outcome Based on Radiomics of Multi-Parametric MRI, AACR 2016.

81. Padhani, Dynamic contrast-enhanced MRI in clinical oncology: current status and future directions, J Magn Reson Imaging. 2002 Oct;16(4):407-22

82. Parekh et al, Multiparametric Deep Learning Tissue Signatures for a Radiological Biomarker of Breast Cancer: Preliminary Results, Division of Cancer Imaging, The Johns Hopkins University School of Medicine. Preprint

83. Parker, Image Reconstruction in Radiology, CRC, 1990

84. Parkins, Investigating the Mechanisms of Breast Cancer Metastasis Using Multimodality Molecular Imaging, PhD Thesis, The University of Western Ontario, 2019

85. Petralia and Thoeny, DW-MRI of the urogenital tract: applications in oncology, Cancer Imaging (2010) 10, S112S123

86. Phelps, PET, Physics, Instrumentation and Scanners, Springer, 2010

87. Poggio et al, Complexity control by gradient descent in deep networks, Nature Communications volume 11, Article number: 1027 (2020)

88. Rizzo et al, Radiomics: the facts and the challenges of image analysis, European Radiology Experimental (2018) 2:36

89. Royle, The Digital Cell, CSHL Press, 2020.

90. Rumelhart et al, Parallel Distributed Processing, Vol 1 and 2, MIT Press, 1986

91. Saha, Basics of PET Imaging, 2nd Ed, Springer, 2010

92. Sanchez, TI-RADS classification of thyroid nodules based on a score modified according to ultrasound criteria for malignancy, Rev. Argent. Radiol. 2014;78(3): 138-148

93. Schreier et al, A Full-Image Deep Segmenter for CT Images in Breast Cancer Radiotherapy Treatment, Front in Onc, July 2019

94. Sencha and Patrunov, Thyroid Ultrasound, Springer, 2019

95. Shah and Zhou, Prostate Biopsy Interpretation: An Illustrated Guide, Springer, 2012

96. Shen and Rubin, Prostate Cancer, CSHL Press, 2019

97. Simon, The Sciences of the Artificial, MIT Press, 1969

98. Stabile et al, Multiparametric MRI for prostate cancer diagnosis: current status and future directions, Nature Rev Urology, July 17, 2019

99. Stattin et al, Improving the Specificity of Screening for Lethal Prostate Cancer Using Prostate-specific Antigen and a Panel of Kallikrein Markers: A Nested Case–Control Study, Euro Urology, 2015

100. Stoyanova et al, Association of multiparametric MRI quantitative imaging features with prostate cancer gene expression in MRI-targeted prostate biopsies, Oncotarget, Vol. 7, No. 33, 2016

101. Stoyanova et al, Prostate Cancer Radiomics and the promise of Radiogenomics, Transl Cancer Res 2016;5(4):432-447

102. Su et al, A Neural-Network-Based Approach to White Blood Cell Classification, The Scientific World Journal, Volume 2014

103. Su, Prostate, Saunders, 2010

104. Subramaniam, Neural Network with Bee Colony Optimization for MRI Brain Cancer Image Classification, The International Arab Journal of Information Technology, March 2015

105. Sun et al, Deep Learning vs. Radiomics for Predicting Axillary Lymph Node Metastasis of Breast Cancer Using Ultrasound Images: Don't Forget the Peritumoral Region, Frontiers in Oncology, January 2020 | Volume 10 | Article 53

106. Supe et al, Image Segmentation and Classification for Medical Image Processing, International Journal on Future Revolution in Computer Science & Communication Engineering Volume: 5 Issue: 1 45 – 52, Jan 2019

107. Tan et al, Thyroid imaging reporting and data system combined with Bethesda classification in qualitative thyroid nodule diagnosis, Medicine (2019) 98:50

108. Tessler et al, ACR Thyroid Imaging, Reporting and Data System (TI-RADS): White Paper of the ACR TI-RADS Committee, Journal of the American College of Radiology, Volume 14, Number 5, May 2017

109. Thamilselvan and Sathiaseelan, Detection and Classification of Lung Cancer MRI Images by using Enhanced K Nearest Neighbor Algorithm, Indian Journal of Science and Technology, Vol 9(43), November 2016

110. Thestrup et al, Biparametric versus multiparametric MRI in the diagnosis of prostate cancer, Acta Radiologica Open, 5 1–8, 2016

111. Türkbey et al, Diffusion-weighted MRI for detecting and monitoring cancer: a review of current applications in body imaging, Diagn Interv Radiol 2012; 18:46–59

112. Volinia et al, A microRNA expression signature of human solid tumors defines cancer gene targets, PNAS February 14, 2006 vol. 103 no. 7 2257–2261

113. Wang et al, Artificial Intelligence in Ultrasound Imaging: Current Research and Applications, Advanced Ultrasound in Diagnosis and Therapy 2019;03:053–061

114. Wang et al, Computer Aided-Diagnosis of Prostate Cancer on Multiparametric MRI: A Technical Review of Current Research, BioMed Research International, Volume 2014, Article ID 789561

115. Wang et al, Computer Aided-Diagnosis of Prostate Cancer on Multiparametric MRI: A Technical Review of Current Research, BioMed Research International, Volume 2014, Article ID 789561

116. Westbrook and Talbot, MRI in Practice, 5th Ed, Wiley, 2019

117. Westbrook, MRI Technique, 4th Ed, Wiley, 2014

118. Westphalen et al, Detection of clinically significant prostate cancer with PIRADS v2 scores, PSA density, and ADC values in regions with and without mpMRI visible lesions, IBJU, Vol. 45 (4): 713-723, July - August, 2019

119. Widrow et al, The No-Prop algorithm: A new learning algorithm for multilayer neural networks, Neural Networks 37 (2013) 182–188

120. Winfield et al, DCE-MRI, DW-MRI, and MRS in Cancer: Challenges and Advantages of Implementing Qualitative and Quantitative Multi-parametric Imaging in the Clinic, Topics in Magnetic Resonance Imaging, Volume 25, Number 5, October 2016

121. Winston, Artificial Intelligence, 2nd Ed, Addison Wesley 1984

122. Yang et al, Magnetic resonance imaging (MRI)-based radiomics for prostate cancer radiotherapy, Transl Androl Urol 2018;7(3):445-458

123. Zhang, et al, An imaging-based approach predicts clinical outcomes in prostate cancer through a novel support vector machine classification, Oncotarget, Vol. 7, No. 47, Aug 2016

8 INDEX

% Free PSA, 23
4K, 36, 37, 38, 39
ADC, 43, 46, 47, 52, 56, 57, 60, 85
algorithm, 5, 24, 28, 29, 52, 85
angiogenesis, 52, 53, 68, 74
AUC, 7, 8, 24, 25, 37, 38, 39, 40, 46, 52
backward propagation, 28
basal, 16, 48, 51, 52, 65, 77
Bayesian Classifier, 15
benign, 6, 19, 24, 28, 42, 44, 45, 48, 53, 59, 68
biomarker, 20
biopsy, 6, 14, 16, 25, 37, 41, 46, 49, 51, 53, 57
BRAFV600E, 68
breast, 14, 20, 32, 50, 51, 52, 53, 54, 56, 57, 58, 59, 60, 80, 81
Calcifications, 15
calcium, 14, 68, 69, 75
cancer, 6, 16, 17, 18, 20, 21, 23, 32, 33, 36, 41, 44, 45, 46, 47, 49, 51, 52, 53, 57, 58, 59, 60, 72, 73, 74, 75, 76, 78, 80, 81, 82, 84, 85
CAT, 15, 16
classifier, 5, 7, 8, 15, 25, 26, 27, 52, 59
clinical, 20, 41, 51, 52, 53, 59, 60, 68, 77, 80, 85
CNN, 57, 58, 59, 65
collagen, 66, 69, 73
cystic, 14
cytological, 4, 16, 17, 36, 65, 77
cytology, 12, 60
DCE, 43, 45, 46, 51, 52, 53, 56, 57, 58, 59, 77, 81, 85
Decision Tree, 15
Deep learning networks, 60
diagnosis, 4, 5, 13, 16, 18, 20, 41, 45, 46, 51, 53, 57, 65, 71, 72, 80, 81, 84
DIC, 50
diffuse, 43, 44, 49, 80
discriminate, 29, 57
DNA, 32, 78
doppler, 14
DWI, 41, 43, 44, 45, 46, 52, 59
dynamic contrast enhancement, 43, 44
E-cadherin, 66, 68
Eikonomics, 4, 13
ERK1/2, 68
exosomes, 34
expression, 33
follicle, 66, 67
follicular, 65, 71, 72, 73
Fourier, 15, 16
Gaussian, 25, 26
gene, 33, 49, 74, 75, 78, 84
genomics, 4, 13, 53, 60, 65, 81
Gleason, 44, 81
Government, 36
heart, 13, 14
HER2, 51, 52, 80
heterogeneous, 42, 43, 60
HGPIN, 6, 16, 17
high-grade, 52
histological, 4, 16, 18, 36, 59, 65, 69, 70, 77
hyperplasia, 42, 44, 75
image, 4, 5, 12, 19, 20, 28, 36, 44, 45, 46, 52, 59, 64, 65, 79
imaging, 4, 5, 12, 13, 14, 16, 19, 20, 41, 42, 43, 45, 46, 49, 51, 52, 53, 57, 58, 59, 77, 80, 82, 84, 85
Least Square Estimate, 29
lenticular, 42
linear classifier, 25
Linear Classifier, 15
linear discriminant, 24
liquid biopsy, 21
luminal, 16, 48, 51, 52, 65
lymph, 57, 58, 68, 72
malignant, 5, 6, 7, 9, 19, 24, 28, 34, 35, 45, 53, 56, 57, 60, 67
MEK1/2, 68
melanoma, 16, 17
metastasis, 33, 34
metastatic, 32, 68, 75

miRNA, 21, 25, 27, 33, 34, 35, 78
Morphology, 15
mpMRI, 12, 14, 19, 20, 41, 44, 45, 49, 51, 85
MRI, 12, 16, 19, 41, 45, 46, 47, 49, 51, 52, 53, 56, 57, 58, 59, 80, 81, 82, 83, 84, 85
mRNA, 34
multidimensional, 21
multifocal, 44
muscle, 7, 61
neural net, 6, 29
neural networks, 4, 13, 27, 29, 57, 59, 60, 82, 85
Neuroendocrine, 73
nodes, 68
nodule, 5, 7, 42, 44, 77, 84
nucleolus, 16
nucleus, 16, 21, 32, 34, 68, 70, 71, 77
optimum, 36
Orphan Annie, 21, 70
ovaries, 14
papilla, 21, 66, 67, 68
papillary, 17, 18, 65, 67, 68, 69, 70, 71, 72, 73
pathognomonic, 13, 21
pathologist, 17
Pattern recognition, 21
PCa, 7, 8, 16, 24, 25, 37, 41, 45, 46, 47, 65
peripheral zone, 43, 44
PET, 81, 84
PI-RADS, 41, 42, 43, 44, 45, 77
pixel, 15, 30
polygenomic, 32
Principal Component Analysis, 26
probability, 6, 7, 9, 10, 26, 37, 38, 39, 40, 45, 47, 72
prognosis, 4, 5, 16, 58, 68
prognostic, 35
prostate, 6, 14, 16, 17, 19, 21, 23, 39, 41, 42, 43, 44, 45, 46, 47, 49, 73, 74, 81, 84, 85
PSA, 6, 12, 14, 23, 24, 25, 26, 36, 37, 39, 40, 85
PSA velocity, 23
PSA Velocity, 24
psammoma, 69
radiologist, 5, 6, 15, 20, 51, 59
Radon, 15
RECIST, 20, 81
RNA, 33, 78
sagittal, 16
sensitivity, 24, 25
specificity, 24, 25
steepest descent, 30
T2-weighted, 41, 44, 45, 46, 53, 59
Texture, 15
thyroid, 5, 7, 14, 16, 17, 60, 61, 66, 68, 69, 72, 73, 75, 76, 77, 80, 84
TI-RADS, 62, 77, 84, 85
train, 29
transcription, 34
transition zone, 41, 42, 43
translation, 34
tumor, 32, 45, 46, 49, 51, 52, 53, 57, 58, 65, 68, 69, 72, 75, 78, 80
tumour, 20, 32
ultrasound, 4, 5, 6, 7, 12, 14, 46, 51, 53, 57, 58, 60, 61, 68, 77, 84
US, 14, 15, 19, 48, 61, 63, 65